

# Structure of neutrino mass matrix and CP violation

Michele Frigerio \*

*INFN, Section of Trieste and International School*

*for Advanced Studies (SISSA), Via Beirut 4, I-34014 Trieste, Italy.*

Alexei Yu. Smirnov †

*The Abdus Salam International Center for Theoretical Physics (ICTP), I-34100 Trieste, Italy*

*and Institute for Nuclear Research, Russian Academy of Sciences, Moscow, Russia.*

## Abstract

We reconstruct the neutrino mass matrix in the flavor basis, using all available experimental data on neutrino oscillations. Majorana nature of neutrinos, normal mass hierarchy (ordering) and validity of the LMA MSW solution of the solar neutrino problem are assumed. We study dependences of the mass matrix elements,  $m_{\alpha\beta}$ , on the CP violating Dirac,  $\delta$ , and Majorana,  $\rho$ ,  $\sigma$ , phases, for different values of the mixing angle  $\theta_{13}$  and of the absolute mass scale,  $m_1$ . The contours of constant mass in the  $\rho - \sigma$  plane have been constructed for all  $m_{\alpha\beta}$ . Possible structures of the mass matrix have been analyzed. We identify regions of parameters in which the matrix has (i) a structure with the dominant  $\mu\tau$ -block, (ii) various hierarchical structures, (iii) structures with special ordering or equalities of elements, (iv) the democratic form. In certain cases the matrix can be parameterized by powers of a unique expansion (ordering) parameter  $\lambda \approx 0.2 - 0.3$  ( $\lambda_{ord} \approx 0.6 - 0.7$ ). Perspectives to further restrict the structure of mass matrix in future experiments, in particular in the  $\beta\beta_{0\nu}$ -decay searches, are discussed.

Ref.SISSA 17/2002/EP

hep-ph/0202247

PACS number: 14.60.Pq, 11.30.Er, 23.40.-s

---

\*frigerio@he.sissa.it

†smirnov@ictp.trieste.it

# 1 Introduction

Significant amount of information about neutrino masses and mixing has already been obtained from experiments on the atmospheric [1] and solar neutrinos [2, 3]. New results are expected soon. What are implications of the existing results for the fundamental theory? What is the mechanism of generation of neutrino mass, the origin of large lepton mixing, the relation between the quark and the lepton masses? The neutrino masses and mixing appear from diagonalization of the neutrino mass matrix. So, the questions we are asking should be considered in terms of properties of the mass matrix. It is expected that the structure of the mass matrix is explained by certain (broken) symmetry realized in certain basis at some high mass scale [4]. We will call this basis the *symmetry basis*. Thus, to approach the fundamental theory, one should find the mass matrix in the symmetry basis and at the corresponding *symmetry scale*. Both abelian (*e.g.*, [5, 6]) and non abelian (*e.g.*, [7]) symmetries, broken (spontaneously) at the various symmetry scales, have been widely considered (see also the reviews [8, 9]). In particular, the possibilities have been studied to identify the flavor symmetry scale with other known scales in the theory like the Grand Unification scale or the string scale.

The first step to the fundamental theory is the reconstruction of the matrix in the *flavor basis* using all available experimental data. The flavor basis, formed by  $\nu_e, \nu_\mu, \nu_\tau$ , is determined as the basis in which the mass matrix of charge leptons is diagonal. However, the symmetry basis may not coincide with the flavor basis, while the structure of the mass matrix depends on the basis substantially. Furthermore, using the existing experimental information we can reconstruct the mass matrix at the low (electroweak) scale. The scale at which possible flavor symmetry is realized (broken) is unknown. So, the bottom-up approach would consist of determination of the structure of the mass matrix at low scale, selection of the appropriate symmetry basis and selection of the correct symmetry scale.

There is a number of attempts to reconstruct neutrino mass matrix in the flavor basis using the available experimental results [10, 11, 12]. Most of the studies have been performed in the context of three Majorana neutrinos and the data on atmospheric and solar neutrinos as well as from the CHOOZ experiment [13] have been used as an input. Clearly this information is not enough to reconstruct the mass matrix. Apart from the oscillation parameters (mass squared differences and mixing angles), the mass matrix depends on non-oscillation parameters: the absolute mass scale,  $m_1$ , and the CP violating Majorana phases. Furthermore, even not all the oscillation parameters are known. In particular, there is only an upper bound on the mixing angle  $\theta_{13}$  and there is no information about

the value of the Dirac phase  $\delta$ . Also the type of mass hierarchy (ordering) of the states is unknown.

The studies performed so far were concentrated, mainly, on identification of the dominant structures of the mass matrix and possible zeros of certain matrix elements. It was realized that in the case of spectrum with normal mass hierarchy,  $m_1 \ll m_2 \ll m_3$ , the mass matrix has structure with dominant  $\mu\tau$ -block, formed by  $M_{\mu\mu}, M_{\mu\tau}, M_{\tau\tau}$  elements, and small elements of the  $e$ -row ( $M_{ee}, M_{e\mu}, M_{e\tau}$ ) [11, 14]. In the case of inverted mass hierarchy, the dominant structure can be formed by the elements of the  $e$ -row:  $M_{e\mu}$  and  $M_{e\tau}$  [6, 10]. These structures may be related to an underlying  $L_e - L_\mu - L_\tau$  symmetry.

In the case of degenerate mass spectrum new dominant structures appear depending on the CP-parities of the mass eigenstates (see, *e.g.*, [6, 10, 15]). In particular, it was found that the diagonal elements, being equal to each other, can form the dominant structure for equal CP-parities of all three neutrinos. Another interesting possibility is the dominant structure formed by the  $ee$ -,  $\mu\tau$ - and  $\tau\mu$ -elements (moreover,  $|M_{ee}| \approx |M_{\mu\tau}|$ ), which could imply, *e.g.*,  $SO(3)$  flavor symmetry or  $U(1)$  symmetry, with charge prescription  $(0, 1, -1)$  and an additional permutation symmetry. Recently, the possibility to have some matrix elements equal to zero has been considered [16].

It was shown that experimental data can be explained in models with universal Yukawa couplings [17], which lead to democratic mass matrices with all mass matrix elements having the same modulus but different phases.

Completely different approach is based on “Anarchy” of the mass matrix [18]. It has been proposed that the elements of the mass matrix appear as random numbers from certain interval and there is no special structure of the mass matrix dictated by certain symmetry. It was estimated how frequently neutrino oscillation data can be reproduced in this way. Random values of CP violating phases have also been considered [11].

It was realized that the structure of the mass matrix may depend strongly on the unknown CP violating phases, especially in the case of degenerate spectrum. In general, in the system of three Majorana neutrinos there are three CP violating phases: the Dirac phase,  $\delta$ , the unique phase in the mixing matrix relevant for oscillations, and two Majorana phases, which are relative phases of the three mass eigenstates.

In most of previous studies, the CP violating phases were neglected and CP-parities have been discussed mainly (see, however, [16] and also [19], where the role of phases in the generation of large solar mixing is considered).

In this paper, we perform a systematic study of dependence of the neutrino mass

matrix structure on the CP violating phases. In section 2 we describe our approach and summarize physical inputs from neutrino oscillation experiments. In sections 3 and 4, we study the dependence of the mass matrix elements on CP violating phases. We consider spectra with mass hierarchy (section 3.1), partial degeneracy (section 4.2) and complete degeneracy (section 4.3). In section 5 we introduce and describe the  $(\rho - \sigma)$  plots. In section 6 we consider implications of CP violating phases for the structure of the mass matrix. In section 7 we discuss our result and draw conclusions.

## 2 Reconstructing $\nu$ mass matrix

### 2.1 Mass matrix in flavor basis

The neutrino mass matrix in flavor basis,  $M$ , can be written as

$$M = U^* M^{diag} U^\dagger , \quad (1)$$

where

$$M^{diag} \equiv \text{Diag}(m_1 e^{-2i\rho}, m_2, m_3 e^{-2i\sigma}) . \quad (2)$$

Here  $m_i$  are the moduli of neutrino mass eigenvalues and  $\rho$  and  $\sigma$  are the two CP violating Majorana phases, varying between 0 and  $\pi$  (in contrast with previous works, we ascribe the phases to the first and the third mass eigenstates, which is more convenient in our approach). The neutrino mixing matrix  $U$  is defined by

$$\nu_{\alpha L} = U_{\alpha i} \nu_{iL} , \quad \alpha = e, \mu, \tau , \quad i = 1, 2, 3 ,$$

where  $\nu_\alpha$  are the flavor neutrino states, and  $\nu_i$  are the mass eigenstates. We use the standard parameterization for  $U$ :

$$U = \begin{pmatrix} c_{13}c_{12} & s_{12}c_{13} & s_{13}e^{-i\delta} \\ -s_{12}c_{23} - s_{23}s_{13}c_{12}e^{i\delta} & c_{23}c_{12} - s_{23}s_{13}s_{12}e^{i\delta} & s_{23}c_{13} \\ s_{23}s_{12} - s_{13}c_{23}c_{12}e^{i\delta} & -s_{23}c_{12} - s_{13}s_{12}c_{23}e^{i\delta} & c_{23}c_{13} \end{pmatrix} , \quad (3)$$

where  $c_{ij} \equiv \cos \theta_{ij}$ ,  $s_{ij} \equiv \sin \theta_{ij}$  and  $\delta$  is the CP violating Dirac phase. The mixing angles vary between 0 and  $\pi/2$  and  $\delta$  between 0 and  $2\pi$ .

The matrix  $M$  is symmetric and, therefore, completely defined by six elements. According to Eqs.(1,2), they can be written explicitly as

$$M_{\alpha\beta} = (U_{\alpha 1}^* U_{\beta 1}^*) m_1 e^{-2i\rho} + (U_{\alpha 2}^* U_{\beta 2}^*) m_2 + (U_{\alpha 3}^* U_{\beta 3}^*) m_3 e^{-2i\sigma} , \quad \alpha, \beta = e, \mu, \tau . \quad (4)$$

The expression for  $M_{\alpha\beta}$ , in terms of  $m_i, \theta_{ij}, \delta, \rho, \sigma$ , is given in the appendix.

In what follows we will analyze the absolute values of mass matrix elements, denoted by

$$m_{\alpha\beta} \equiv |M_{\alpha\beta}|, \quad \alpha, \beta = e, \mu, \tau.$$

Notice that, in flavor basis,  $m_{\alpha\beta}$  are physical quantities, that is, they can be *directly* measured in physical processes. In particular, the rate of the neutrinoless  $2\beta$ -decay is proportional to  $m_{ee}^2$ . Other entries are in principle measurable in processes with  $\Delta L = 2$ , like the decay  $K^+ \rightarrow \pi^- \mu^+ \mu^+$  or the scattering  $e^- p \rightarrow \nu_e l^\pm l'^\pm X$  (for a review see [20]). The rates of these processes are proportional to  $m_{\alpha\beta}^2$ , where  $\alpha$  and  $\beta$  are the flavors of the two produced leptons in the final state or leptons in the initial and final states).

We introduce the dimensionless quantities

$$\tilde{M}_{\alpha\beta} \equiv \frac{M_{\alpha\beta}}{m_3}, \quad \tilde{m}_{\alpha\beta} \equiv \frac{m_{\alpha\beta}}{m_3},$$

where  $m_3$  is the largest mass eigenvalue.

## 2.2 Conservation of the sum of masses squared

According to (1), the mixing matrix distributes the masses from  $M^{diag}$  to the elements of the flavor mass matrix  $M$ :

$$m_1, m_2, m_3 \rightarrow m_{\alpha\beta}.$$

The following sum rule is useful for analysis of the flavor mass matrix:

$$S_0 \equiv \sum_{i=1,2,3} m_i^2 = \sum_{\alpha,\beta=e,\mu,\tau} m_{\alpha\beta}^2. \quad (5)$$

That is, the sum of moduli squared of all the elements of the mass matrix is invariant under basis transformation (rotation). The equality (5) is the straightforward consequence of the unitarity of transformation. Indeed, denoting  $M_i \equiv M_i^{diag}$  ( $|M_i| \equiv m_i$ ), we can write, using Eqs.(1,2):

$$\begin{aligned} \sum_{\alpha,\beta} m_{\alpha\beta}^2 &= \sum_{\alpha,\beta} \left| \sum_i U_{\alpha i}^* U_{\beta i} M_i \right|^2 = \\ &= \sum_i \sum_{\alpha,\beta} |U_{\alpha i}^* U_{\beta i} M_i|^2 + \sum_{i>j} \sum_{\alpha,\beta} [U_{\alpha i}^* U_{\beta i}^* U_{\alpha j} U_{\beta j} M_i M_j^* + h.c.]. \end{aligned}$$

The first term is immediately reduced to  $\sum_i |M_i|^2 = \sum_i m_i^2$ , whereas the second term is zero due to orthogonality:  $\sum_\alpha U_{\alpha i}^* U_{\alpha j} = 0$  for  $i \neq j$ .

## 2.3 Experimental input

In what follows we will find  $m_{\alpha\beta} = m_{\alpha\beta}(m_i, \theta_{ij}, \delta, \rho, \sigma)$ , using all available neutrino data. We will restrict our analysis to the case of normal mass hierarchy (ordering):  $m_1 \ll m_2 \ll m_3$  ( $m_1 < m_2 < m_3$ ). The inverted hierarchy (ordering) is disfavored by supernova SN1987A data [21] (see, however, [22]). Normal hierarchy implies that  $m_2^2 - m_1^2 \equiv \Delta m_{sol}^2$  and  $m_3^2 - m_2^2 \simeq m_3^2 - m_1^2 \equiv \Delta m_{atm}^2$ . We will also restrict ourselves to the LMA MSW solution of the solar neutrino problem, which gives the best global fit of the solar neutrino data [23]. This solution looks especially plausible after SNO data [3] and it can be tested in the already operating KamLAND experiment [24]. We accept interpretation of the atmospheric neutrino results [1] in terms of  $\nu_\mu \rightarrow \nu_\tau$  oscillations as the dominant mode.

The following experimental information is used.

- The best fit point for the LMA solution [23]:

$$\tan^2 \theta_{12} = 0.36, \quad \Delta m_{sol}^2 = 5 \cdot 10^{-5} \text{eV}^2 . \quad (6)$$

At 99% C.L. the following intervals are allowed:

$$\tan^2 \theta_{12} = 0.20 - 0.93, \quad \Delta m_{sol}^2 = (2 - 50) \cdot 10^{-5} \text{eV}^2 . \quad (7)$$

- From atmospheric neutrino analysis we take, at the 99% C.L. [1]:

$$\tan \theta_{23} = 1_{-0.35}^{+0.54}, \quad \Delta m_{atm}^2 = (2.5_{-1.3}^{+2.5}) \cdot 10^{-3} \text{eV}^2 . \quad (8)$$

- We use the CHOOZ bound on  $\theta_{13}$  at the 90% C.L. [13]:

$$\sin \theta_{13} \lesssim 0.22 \quad (\Delta m_{atm}^2 \gtrsim 2 \cdot 10^{-3} \text{eV}^2). \quad (9)$$

In our discussion we will take into account the upper limit on the Majorana neutrino mass from neutrinoless  $2\beta$  decay [26, 27]:

$$m_{ee} < 0.35 \text{ eV} \quad (90\% \text{ C.L.}) , \quad (10)$$

and  $m_{ee} \lesssim 1 \text{ eV}$ , if uncertainties in the nuclear matrix elements are taken into account. It is premature to include in the analysis the recent controversial result on  $2\beta_{0\nu}$ -decay [28] (see discussion in [15, 29]). We consider also the direct kinematic bound on the mass of electron neutrino [25],

$$m_e < 2.2 \text{ eV} \quad (95\% \text{ C.L.}) . \quad (11)$$

We will treat the unknown CP violating phases  $\delta, \rho, \sigma$ , as well as the absolute mass scale,  $m_1$ , and the angle  $\theta_{13}$  as free parameters and we will study the dependence of  $m_{\alpha\beta}$  on their values.

Let us emphasize that the experimental input (6) - (9) does not depend on the Majorana phases,  $\rho$  and  $\sigma$ , and on  $m_1$ , because only the differences of  $m_i^2$  enter the oscillation probabilities. The input does not depend also on the Dirac phase,  $\delta$ . This can be explicitly seen from the parameterization (3): at the level of present experimental accuracy, the solar and atmospheric neutrino results are determined by  $U_{e1}, U_{e2}$  and  $U_{\mu3}, U_{\tau3}$  respectively. CHOOZ gives the bound on  $|U_{e3}|$ . All these quantities do not depend on  $\delta$ .

## 2.4 $\mu\tau$ -block and $e$ -row elements

In view of large 2-3 mixing, it is convenient to split the six independent elements of the mass matrix into three groups:

- elements of the  $\mu\tau$ -block:  $m_{\mu\mu}, m_{\mu\tau}, m_{\tau\tau}$ , with zero electron lepton number,  $L_e = 0$ ;
- elements of the  $e$ -row with  $L_e = 1$ :  $m_{e\mu}, m_{e\tau}$ ;
- element of the  $e$ -row with  $L_e = 2$ :  $m_{ee}$ .

As we will see later, these groups of elements have different dependences on CP violating phases. Moreover, such a split can be motivated by phenomenology.

## 2.5 Small parameters and limits

There are several small parameters which can be used to study properties of the mass matrix:

- 1) The ratio of masses  $m_2/m_3$  is a small parameter in the case of mass hierarchy:

$$r \equiv \frac{m_2}{m_3} \approx \sqrt{\frac{\Delta m_{sun}^2}{\Delta m_{atm}^2}}.$$

For best fit values of mass squared differences (see (6),(8)) and  $m_1 \approx 0$ , the ratio equals  $r = 0.14$ ; varying  $\Delta m_{atm}^2$  and  $\Delta m_{sol}^2$  in the ranges given in (8) and (7), one gets  $0.06 \lesssim r \lesssim 0.6$ ;

- 2) The 1-3 mixing:  $s_{13} \lesssim 0.2$  (see (9));
- 3) The deviation of 2-3 mixing from maximal value (see (8)), which can be described by

$$\xi \equiv \cos 2\theta_{23} \sim (-0.4 \div 0.4).$$

Future experimental studies can further restrict all these three parameters.

Let us introduce also another dimensionless parameter:

$$k \equiv \frac{m_1}{m_2} .$$

In the case of normal mass hierarchy,  $k \approx 0$ . Clearly, we may have  $k \sim 1$  and  $r \ll 1$ . If  $r \sim 1$ , then  $k \approx 1$ .

Let us consider the mass matrix in various limits.

1)  $r = s_{13} = \xi = 0$ . In this case we arrive at a matrix with zero  $e$ -row elements and  $\mu\tau$ -block elements equal to  $m_3/2$ . Obviously no dependence on CP-phases appears.

2)  $r = s_{13} = 0$ ,  $\xi \neq 0$  (see (A.4)-(A.6)). We get

$$\tilde{m}_{\mu\mu} = \frac{1}{2}(1 - \xi) , \quad \tilde{m}_{\tau\tau} = \frac{1}{2}(1 + \xi) , \quad \tilde{m}_{\mu\tau} = \frac{1}{2}\sqrt{1 - \xi^2} . \quad (12)$$

The element  $m_{\mu\tau}$  is almost unchanged with respect to maximal  $\theta_{23}$ , while  $m_{\mu\mu}$  and  $m_{\tau\tau}$  vary with  $\xi$  significantly and in opposite directions. The determinant of the  $\mu\tau$ -block is zero. Again, there is no dependence on CP violating phases.

3)  $s_{13} = \xi = m_1 = 0$ , but  $r \neq 0$ . We have

$$M = \frac{m_3}{2} \begin{pmatrix} 2s_{12}^2 r & \sqrt{2}s_{12}c_{12}r & -\sqrt{2}s_{12}c_{12}r \\ \dots & e^{-2i\sigma} + c_{12}^2 r & e^{-2i\sigma} - c_{12}^2 r \\ \dots & \dots & e^{-2i\sigma} + c_{12}^2 r \end{pmatrix} . \quad (13)$$

Now dependence on the Majorana phase appears in the  $\mu\tau$ -block, but there is no phase dependence of the  $e$ -row elements. In the hierarchical case,  $r \ll 1$ , the phase  $\sigma$  does not change the structure of the mass matrix substantially. The influence of the CP violating phases on the matrix structure is very weak in the limit of strong mass hierarchy and small  $s_{13}$ . The dependence of the elements on the Dirac phase is associated with  $s_{13}$ , so the effect of  $\delta$  increases with  $s_{13}$ , while the dependence on the phase  $\rho$  is associated to the mass  $m_1$  and it is negligible in the strong hierarchy case.

## 2.6 Analytic expressions and phase diagrams

Exact analytic expressions for the mass matrix elements in terms of mass eigenvalues,  $m_i$ , mixing angles and phases are given in the Appendix. We present the matrix elements as sums of three contributions corresponding to three different mass eigenvalues in (A.1 - A.6) and as series in powers of  $s_{13}$  (A.7). Representation of  $m_{\alpha\beta}$  as the sums of three terms with different phases is given in (A.9, A.11, A.13). We will use various approximate expressions for  $m_{\alpha\beta}$  which can be obtained from Eqs.(A.1 - A.13).



For small  $s_{13}$ , one can draw simple graphic representation of the mass matrix elements in the complex plane (Fig.1). Indeed, neglecting terms of order  $s_{13}$  in the brackets of Eqs.(A.2 - A.6) or, equivalently,  $\epsilon$  terms in Eqs.(A.9, A.11), we find that each mass  $m_{\alpha\beta}$  turns out to be the sum of three terms with phase factors which depend on certain combinations of the phases  $\delta, \rho, \sigma$ . So, the masses  $m_{\alpha\beta}$  can be represented in the complex plane as sums of three vectors (corresponding to the three terms). The lengths of these vectors are determined by mass eigenvalues (ratios  $k$  and  $r$ ) and mixing angles. The angles between vectors are given by combinations of the phases  $\delta, \rho, \sigma$ .

We will call this representation, first suggested in [30] for  $m_{ee}$ , the *phase diagram*. The phase diagrams allow one easily to find minimal and maximal values of the matrix elements and possible correlations between them. In Fig.1 we show phase diagrams for the case of partial degeneracy:  $k \approx 1$ ,  $r \lesssim 1$ .

The mass matrix elements are periodic functions of the CP violating phases. In what follows we will study these dependences by quantifying for each phase the amplitude of variations, the period and the average value of the element. The latter we define as the average between maximal and minimal possible value of the element. We will also consider the relative phases of variations of different elements and correlations between them.

### 3 CP phases in the case of hierarchical mass spectrum

In the limit of strong mass hierarchy, when  $m_1 \approx 0$ ,  $m_2^2 \approx \Delta m_{sol}^2$  and  $m_3^2 \approx \Delta m_{atm}^2$ ,  $k \approx 0$ , only one Majorana phase  $\sigma$  is relevant. In the limit  $s_{13} \approx 0$ , we have, for the matrix of the moduli:

$$\tilde{m} = \begin{pmatrix} s_{12}^2 r & c_{23} s_{12} c_{12} r & s_{23} s_{12} c_{12} r \\ \dots & |c_{12}^2 c_{23}^2 r + s_{23}^2 e^{-2i\sigma}| & s_{23} c_{23} |c_{12}^2 r - e^{-2i\sigma}| \\ \dots & \dots & |c_{12}^2 s_{23}^2 r + c_{23}^2 e^{-2i\sigma}| \end{pmatrix}. \quad (14)$$

#### 3.1 Dependence of $m_{\alpha\beta}$ on CP phases

In Figs.2,3 we show the six mass matrix elements,  $\tilde{m}_{\alpha\beta}$ ,  $\alpha, \beta = e, \mu, \tau$ , as functions of the phase  $\sigma$ , for different values of the mixing angles  $\theta_{23}$  and  $\theta_{13}$ , from the allowed regions given in (8) and (9). Main features of the dependences can be well understood taking the lowest order terms in  $r$  and  $s_{13}$  from Eqs.(A.9,A.11,A.13).

According to (14), the dependence of the  $\mu\tau$ -block elements on  $\sigma$  is a result of the interplay of the main,  $\mathcal{O}(1)$ , term and of the  $\mathcal{O}(r)$  term. In the lowest order, the  $\mu\tau$ -block elements do not depend on  $s_{13}$  (see Figs.2,3). All these elements vary with the same frequency, but  $m_{\mu\tau}$  has an opposite phase with respect to the two other elements. The relative amplitude of variations equals

$$\frac{\Delta m^\sigma}{m} \approx c_{12}^2 r \times \begin{cases} \cot^2 \theta_{23}, & m_{\mu\mu} \\ \tan^2 \theta_{23}, & m_{\tau\tau} \\ 1, & m_{\mu\tau} \end{cases} . \quad (15)$$

The amplitudes are equal for maximal 2-3 mixing. For the best fit values of the parameters they are of order 10%. For non-maximal 2-3 mixing, the amplitudes of variations can reach  $\sim 25\%$ . The corrections  $\sim r s_{13}$  (A.10) lead to small phase shift and small change of the amplitude of variations.

Neglecting terms of order  $r s_{13} s_{12}^2$ , we get from (A.11) expressions for  $m_{e\mu}$  and  $m_{e\tau}$ :

$$\tilde{m}_{e\mu} \approx \left| r s_{12} c_{12} c_{23} + s_{13} s_{23} e^{i(\delta-2\sigma)} \right| , \quad (16)$$

$$\tilde{m}_{e\tau} \approx \left| r s_{12} c_{12} s_{23} - s_{13} c_{23} e^{i(\delta-2\sigma)} \right| . \quad (17)$$

So, the elements  $m_{e\mu}$  and  $m_{e\tau}$  depend on phases in the combination  $(\delta - 2\sigma)$ ; moreover, they change with  $(\delta - 2\sigma)$  in opposite phases. The values of  $m_{e\mu}$  and  $m_{e\tau}$  are determined by the interplay of the order  $r$  and order  $s_{13}$  terms, which can have comparable sizes. Possible maximal values of  $m_{e\mu}$  and  $m_{e\tau}$  increase with  $s_{13}$ .

The relative amplitude of variations of  $m_{e\mu}$  with  $(\delta - 2\sigma)$  is maximal when the two terms in (16) have the same modulus:

$$s_{13} = s_{13}^0 \equiv \frac{1}{2} r \sin 2\theta_{12} \cot \theta_{23} \approx 0.06 . \quad (18)$$

If  $s_{13} = s_{13}^0$ ,

$$m_{e\mu} = 0 \quad \text{for} \quad \delta - 2\sigma = \pi .$$

Maximal value of  $m_{e\mu}$  equals  $m_{e\mu}^{max} = 2\tilde{m}_{e\mu} = \sin 2\theta_{12} c_{23} r$ . For  $s_{13} < s_{13}^0$ , (Fig.2a,2c,2e), the average value of  $m_{e\mu}$  is determined by the first term in (16), whereas the amplitude of variations is given by  $s_{13}/s_{13}^0$ . For  $s_{13} > s_{13}^0$ , the second term in (16) dominates. It determines the average value of  $m_{e\mu}$ , around which variations occur. The relative amplitude of variations is given by the factor  $s_{13}^0/s_{13}$  (Fig.2b,2d,2f).

Behavior of the element  $m_{e\tau}$  is similar: the first and the second terms in (17) have the same modulus at

$$s_{13} = \bar{s}_{13}^0 \equiv \frac{1}{2}r \sin 2\theta_{12} \tan \theta_{23} \quad (19)$$

( $\bar{s}_{13}^0 = s_{13}^0$  for maximal 2-3 mixing). Moreover, the two terms have opposite signs, so that

$$m_{e\tau} = 0 \quad \text{for} \quad \delta - 2\sigma = 0 .$$

For maximal mixing,  $m_{e\mu}$  and  $m_{e\tau}$  can have maximal amplitude of variations simultaneously. Corrections of order  $rs_{13}s_{12}^2$ , neglected in (16) and (17), produce a small relative shift of phases of  $\tilde{m}_{e\mu}$  and  $\tilde{m}_{e\tau}$  (see Fig.2).

For the  $ee$ -element we have:

$$\tilde{m}_{ee} \approx |c_{13}^2 s_{12}^2 r + s_{13}^2 e^{2i(\delta-\sigma)}| . \quad (20)$$

The  $ee$ -element depends on the combination of phases  $2(\delta - \sigma)$ . Due to the factor  $rs_{12}^2$  in the first term, both contributions in (20) can be comparable in spite of the  $s_{13}^2$ -order of the second term. They are equal at  $\tan \theta_{13} = s_{12}\sqrt{r} \approx 0.19$ , that is, near the upper limit for  $s_{13}$ . In this case the amplitude of variation can be maximal and

$$m_{ee} = 0 \quad \text{for} \quad \delta - \sigma = \pi/2, 3\pi/2 .$$

Such a situation is approximately realized in Fig.2b,2d,2f. For small values of  $s_{13}$  ( $s_{13} \ll 0.2$ ), the dependence of  $m_{ee}$  on phases is negligible (Fig.2a,2c,2e). The relative amplitude of variations is determined by the ratio  $\tan^2 \theta_{13}/(rs_{12}^2)$  and the average value equals  $\bar{m}_{ee} \approx s_{12}^2 r$ .

Let us analyze the dependence of matrix elements on the Dirac phase  $\delta$ . The elements of  $\mu\tau$ -block depend on  $\delta$  very weakly, via order  $rs_{13}$  corrections (see (A.10)). E.g., for  $s_{13} \approx 0.17$  (Fig.2b,2d,2f), we find relative amplitudes of variations  $\Delta m_{\mu\mu}^\delta / \bar{m}_{\mu\mu} \approx \Delta m_{\tau\tau}^\delta / \bar{m}_{\tau\tau} \sim 0.02$ . The dependence of  $m_{\mu\tau}$  on  $\delta$  is further suppressed by the factor  $\xi \equiv \cos 2\theta_{23}$ .

The elements of the  $e$ -row have much stronger relative dependence on  $\delta$ . As we pointed out, the elements  $m_{e\mu}$  and  $m_{e\tau}$  depend on phases in the combination  $(\delta - 2\sigma)$  (this feature is weakly violated by corrections  $\sim rs_{13}$ , which depend on the phase  $\delta$  only). So, up to corrections of order  $s_{13}r$ , one can extract the information on the  $\delta$  dependence of the elements from the Fig.2 (or Fig.3 for large  $r$ ) immediately. The change of  $\delta$  by amount  $\Delta\delta$  is equivalent to horizontally shift the lines which correspond to  $m_{e\mu}$  and  $m_{e\tau}$  along with  $\sigma$ -axis by  $\Delta\delta/2$  and the  $m_{ee}$  line by  $\Delta\delta$ , with respect to the lines of  $\mu\tau$ -block, which are

almost unchanged. The phase  $\delta$  can be selected in such a way that certain features of the  $m_{ee}$  line and other  $e$ -row lines will occur at the same value of  $\sigma$ . For instance, according to Fig.2b, one can get  $\tilde{m}_{ee} \ll \tilde{m}_{e\mu} \ll \tilde{m}_{e\tau}$ .

All the elements have the same period of variation with  $\sigma$ , although the phases of variations are different. There is a phase shift by  $\pi$  within different groups:

$$\phi(\tilde{m}_{\mu\mu}) = \phi(\tilde{m}_{\tau\tau}) = \phi(\tilde{m}_{\mu\tau}) + \pi = -2\sigma ; \quad (21)$$

$$\phi(\tilde{m}_{e\mu}) = \phi(\tilde{m}_{e\tau}) + \pi = -2\sigma + \delta . \quad (22)$$

There is a relative shift of phase between  $\mu\tau$ -block and  $e$ -row elements which is determined by  $\delta$ :

$$\phi(\tilde{m}_{e\mu}) - \phi(\tilde{m}_{\mu\mu}) = \delta , \quad \phi(\tilde{m}_{ee}) - \phi(\tilde{m}_{e\mu}) = \delta . \quad (23)$$

These relations are weakly broken by corrections of order  $rs_{13}$ .

### 3.2 Dependence on $\theta_{12}$ , $r$ and $k$

Variations of  $\theta_{12}$  within the allowed LMA region, given in (7), do not produce drastic changes of results shown in Fig.2. With increase of  $\theta_{12}$ , the amplitude of variations of  $\mu\tau$ -block elements with  $\sigma$  (see (15)) decreases as  $c_{12}^2$ . For maximal 1-2 mixing we get  $\sim (30 - 35)\%$  decrease in comparison with the best fit value of  $\theta_{12}$ . In contrast, the amplitude of variations of these elements with  $\delta$  increases as  $\sin 2\theta_{12}$  (see (A.10)). The dependence on  $\delta$  remains weak, even though the increase of the amplitude can be about  $(30 - 40)\%$ . For the  $e$ -row elements, the critical value  $s_{13}^0$  is proportional to  $\sin 2\theta_{12}$  (see (18)). The  $ee$ -element  $m_{ee}$  can be two times larger for almost maximal solar mixing angle than for the best fit value (see (20)).

Changes of  $\Delta m_{sol}^2$  and  $\Delta m_{atm}^2$  within the allowed regions, (7) and (8), produce strong effect on the structure of the mass matrix. In Fig.3 we show the dependence of mass matrix elements on  $\sigma$  for  $r = 0.3$ , corresponding, *e.g.*, to  $\Delta m_{sol}^2 \approx 2 \cdot 10^{-4} \text{eV}^2$  and  $\Delta m_{atm}^2 \approx 2 \cdot 10^{-3} \text{eV}^2$ . For the  $\mu\tau$ -block elements, the amplitudes increase linearly with  $r$  (see (15)) and for  $r \approx 0.3$  they can be larger than 30%. For the  $e$ -row elements the critical value  $s_{13}^0$  (see (18)) also increases linearly with  $r$ ; for  $r \approx 0.3$ , we get  $s_{13}^0 \approx 0.13$ . For  $s_{13} < s_{13}^0$ , the average values of elements increase as  $m_{e\mu} \sim m_{e\tau} \sim r$ , but the amplitude of variations with  $(\delta - 2\sigma)$  does not change (compare Fig.3, panels a,c,e, with corresponding panels in Fig.2). For  $s_{13} \gtrsim s_{13}^0$ , the average values of  $m_{e\mu}$  and  $m_{e\tau}$  do not depend on  $r$ , while their

amplitudes can be maximal (Fig.3, panels b,d,f). The average value of the  $ee$ -element increases with  $r$ :  $m_{ee} \sim r$ ; the amplitude of variations with  $2(\delta - \sigma)$  does not change.

Till now, we have considered the case  $m_1 = 0$ . A strong normal hierarchy among mass eigenvalues,  $m_1 \ll m_2 \ll m_3$ , holds for  $m_1$  up to approximately 0.002 eV ( $k < 0.3$ ). Notice that, for  $m_1 \neq 0$ , both Majorana phases become relevant (see (4)). We have checked that varying  $m_1$  between 0 and 0.002eV, the dependence of  $m_{\alpha\beta}$  on angles and CP phases, showed in Figs.2,3, is qualitatively the same as for  $m_1 = 0$ , except for the dependence of  $m_{ee}$ . The  $ee$ -element can be about two times larger. Indeed, neglecting terms of order  $s_{13}^2$ , we get:

$$\tilde{m}_{ee} \approx r s_{12}^2 (1 + k \cot^2 \theta_{12} \cos 2\rho) .$$

The second term in the brackets is of order one for, *e.g.*,  $m_1 = 0.002$  eV,  $m_2 = 0.006$  eV,  $\tan^2 \theta_{12} = 0.35$  and  $\rho = 0, \pi$ . Depending on  $\rho$ , the ratio between  $m_{ee}$  and the other  $e$ -row elements can significantly change.

### 3.3 Structure of the mass matrix in the hierarchical case

1) As follows from Figs.2,3, the sharp structure with the dominant  $\mu\tau$ -block and subdominant  $e$ -row appears for small  $s_{13}$ , small  $r$  and near maximal 2-3 mixing. In this case

$$m_{ee} \sim m_{e\mu} \sim m_{e\tau} \ll m_{\mu\mu} \sim m_{\mu\tau} \sim m_{\tau\tau},$$

$$\frac{m(e - \text{row})}{m(\mu\tau - \text{block})} \sim s_{13}, r \sim 0.1, \quad (24)$$

where  $m(e - \text{row})$  and  $m(\mu\tau - \text{block})$  refer to typical masses of the  $e$ -row and  $\mu\tau$ -block elements. Improvements of the upper bound on  $s_{13}$  and on the deviation of 2-3 mixing from maximal value,  $\xi$ , as well as establishing  $\Delta m_{sol}^2$  near its present best fit value, will confirm this structure in assumption of mass hierarchy. In the limit of sharp structure [ $\mu\tau$ -block]-[ $e$ -row], the elements of the dominant block depend very weakly on  $\delta$  and have about 10% variations (determined by  $r$ ) due to the phase  $\sigma$ . The elements  $m_{e\mu}$  and  $m_{e\tau}$  depend significantly on the combination  $(\delta - 2\sigma)$ , unless very strong upper bound on  $s_{13}$  will be established. The  $ee$ -element varies with  $2(\delta - \sigma)$ , with amplitude  $\sim s_{13}^2$ . Thus, uncertainties in the structure of the mass matrix due to unknown CP violating phases can be substantially reduced by further measurements of mixing angles and mass squared differences.

According to Figs.2,3, for a large part of the parameter space  $(\theta_{23}, \theta_{13}, r, \delta, \sigma)$ , the structure  $[\mu\tau\text{-block}]\text{-}[e\text{-row}]$  is less profound or even disappears. Indeed, in the case of significant deviation of the 2-3 mixing from maximal one or/and large enough  $r$ , the split between masses within the  $\mu\tau$ -block can be larger than the gap between  $m(e\text{-row})$  and  $m(\mu\tau\text{-block})$ , depending on  $\sigma$ . In this situation, separation of the elements in two groups loses any sense. For the extreme case of large values of  $r$ , the elements  $m_{e\mu}$  and  $m_{e\tau}$  can be even larger than  $m_{\mu\mu}$  or  $m_{\tau\tau}$ .

2) Dependence of the gap between  $\mu\tau$ -block and  $e$ -row elements on  $s_{13}$  and  $r$  can be seen comparing left and right panels in Figs.2,3 and Fig.2 with Fig.3, respectively. The deviation from maximality of  $\theta_{23}$ , leading to a spread among the  $\mu\tau$ -block elements (see (12)), can strongly decrease the gap.

Let us quantify the gap more strictly. Taking only leading terms in  $\xi$ ,  $r$  and  $s_{13}$ , one has for the  $\mu\tau$ -block elements:

$$m(\mu\tau\text{-block}) \geq m(\mu\tau\text{-block})^{\min} \equiv \frac{m_3}{2}(1 - |\xi| - rc_{12}^2),$$

where  $m(\mu\tau\text{-block})^{\min}$  is the value of  $m_{\mu\mu}$  or  $m_{\tau\tau}$ , for  $\sigma = \pi/2$ . The upper bound on the  $e$ -row elements is given by

$$m(e\text{-row}) \leq m(e\text{-row})^{\max} \equiv \frac{m_3}{\sqrt{2}}(s_{13} + rc_{12}s_{12}),$$

where  $m(e\text{-row})^{\max}$  is the value of  $m_{e\mu}$  or  $m_{e\tau}$ , for  $\delta - 2\sigma = 0$  or  $\pi$ , respectively. Therefore, minimal value of the gap equals

$$m(\mu\tau\text{-block})^{\min} - m(e\text{-row})^{\max} = \frac{m_3}{2} \left[ 1 - |\xi| - r(c_{12}^2 + \sqrt{2}c_{12}s_{12}) - \sqrt{2}s_{13} \right]. \quad (25)$$

One can also characterize the split of the elements by the ratio of mean values of the  $e$ -row and  $\mu\tau$ -block elements. Up to terms quadratic in  $\xi$ ,  $r$  and  $s_{13}$ ,  $\bar{m}(\mu\tau\text{-block}) \approx m_3/2$ , while for the  $e$ -row we can take

$$\bar{m}(e\text{-row}) \equiv \sqrt{\frac{m_{e\mu}^2 + m_{e\tau}^2}{2}} \approx \frac{m_3}{\sqrt{2}}(s_{13}^2 + r^2c_{12}^2s_{12}^2)^{1/2}.$$

Then

$$\frac{\bar{m}(e\text{-row})}{\bar{m}(\mu\tau\text{-block})} \approx \sqrt{2(s_{13}^2 + r^2c_{12}^2s_{12}^2)}, \quad (26)$$

in accordance with (24). The ratio (26) does not depend on CP phases and on  $\theta_{23}$ .

3) Apart from special choice of phases, the  $ee$ -element is typically of the order of the other  $e$ -row elements.

4) The CP violating phases can change significantly the structure of the  $e$ -row. As follows from Figs.2,3, one can get, *e.g.*, a situation where

$$\begin{aligned}
m_{ee} &\ll m_{e\mu} \ll m_{e\tau} && (\text{small } r, \text{ large } s_{13}) ; \\
m_{ee} &\ll m_{e\mu} \approx m_{e\tau} && (\text{small } r, \text{ large } s_{13}) ; \\
m_{ee} &\approx m_{e\mu} \approx m_{e\tau} && (\text{large } r, \text{ small } s_{13}) ; \\
m_{e\mu} &\ll m_{ee} \ll m_{e\tau} && (\text{large } r, \text{ large } s_{13}) .
\end{aligned} \tag{27}$$

Any element of the  $e$ -row can be the smallest one. Depending on phases, all possible orderings of  $e$ -row elements are possible.

5) Depending on phases, one can find a configuration with almost uniform splits among the six mass matrix elements and structure with the dominant  $\mu\tau$ -block disappears. Still the average value of the  $e$ -row elements is smaller than the average value of the  $\mu\tau$ -block elements (see (26)).

## 4 CP phases in the case of non-hierarchical mass spectrum

In what follows we will discuss three possible regions for  $m_1$ :

1.  $m_1 \lesssim \sqrt{\Delta m_{sol}^2}$ , which corresponds to the non-degeneracy case, with  $k \lesssim 1$  and  $r \ll 1$ ;
2.  $\sqrt{\Delta m_{sol}^2} \ll m_1 \lesssim \sqrt{\Delta m_{atm}^2}$ , which is the case of partial degeneracy:  $k \approx 1$ ,  $r \lesssim 1$ ;
3.  $m_1 \gg \sqrt{\Delta m_{atm}^2}$ , which implies complete degeneracy of the spectrum:  $k \approx r \approx 1$ .

With respect to the hierarchical case, the structure of the mass matrix depends on two additional parameters: the mass ratio  $k$  and the relative phase between first and second mass eigenvalues,  $\rho$ . These parameters enter the mass matrix elements in the combinations (see (A.7))

$$X \equiv s_{12}^2 k e^{-2i\rho} + c_{12}^2, \quad Y \equiv s_{12} c_{12} (1 - k e^{-2i\rho}), \quad Z \equiv c_{12}^2 k e^{-2i\rho} + s_{12}^2 \tag{28}$$

(in the hierarchical case,  $k \approx 0$ ,  $X \approx c_{12}^2$ ,  $Y \approx s_{12} c_{12}$  and  $Z \approx s_{12}^2$ ). We will use the following parameterization:

$$X \equiv x e^{i\phi_X}, \quad Y \equiv y e^{i\phi_Y}, \quad Z \equiv z e^{i\phi_Z}, \tag{29}$$

where  $x \equiv |X|$ ,  $\phi_X$ ,  $y \equiv |Y|$ ,  $\phi_Y$ ,  $z \equiv |Z|$ ,  $\phi_Z$  are functions of  $\theta_{12}$ ,  $k$  and  $\rho$ .

Again, it is worthwhile to write the matrix of the absolute values in the limit of very small  $s_{13}$  and then consider corrections due to terms of order  $s_{13}$ . Using (A.7) and the notation (29), we have:

$$\tilde{m} = \begin{pmatrix} rz & c_{23}ry & s_{23}ry \\ \dots & |c_{23}^2rx + s_{23}^2e^{-2i\sigma_X}| & s_{23}c_{23}| - rx + e^{-2i\sigma_X}| \\ \dots & \dots & |s_{23}^2rx + c_{23}^2e^{-2i\sigma_X}| \end{pmatrix}, \quad (30)$$

where  $\sigma_X \equiv \sigma + \phi_X/2$ .

## 4.1 Non-degeneracy case

For  $m_1 \lesssim \sqrt{\Delta m_{sol}^2}$ , we have  $k \lesssim 1$ . The largest mass is still given by  $m_3 \approx \sqrt{\Delta m_{atm}^2}$ . The contributions of  $m_1$  to the  $\mu\tau$ -block elements appear as small corrections, but they can be of order 1 for the  $e$ -row elements.

Neglecting terms of order  $s_{13}$ , we can use for the  $\mu\tau$ -block elements the expressions in (30). Comparing with the hierarchical case (see Eq.(14)), we find that the effect of  $m_1$  on the elements of  $\mu\tau$ -block is reduced to renormalization of the mass ratio  $r$  and shift of the phase  $\sigma$ :

$$r \rightarrow r_X \equiv r \frac{x}{c_{12}^2}, \quad \sigma \rightarrow \sigma_X \equiv \sigma + \frac{1}{2}\phi_X. \quad (31)$$

So, one can find dependence of the elements on phases from Figs.2,3, by appropriate change of  $r$  and  $\sigma$ .

Depending on the phase  $\rho$ , the contribution related to  $m_1$  can suppress or enhance the amplitude of variations of  $\mu\tau$ -block elements with  $\sigma$  (see (15)). The extreme modifications are determined by

$$r_X = \begin{cases} r(1 + k \tan^2 \theta_{12}), & \text{for } \rho = 0 \\ r(1 - k \tan^2 \theta_{12}), & \text{for } \rho = \pi/2 \end{cases}.$$

For  $k \lesssim 1$  and  $\tan^2 \theta_{12} \lesssim 0.5$ , the relative effect of  $m_1$  is below 50%. For  $\rho = 0, \pi/2$ , we have  $\phi_X = 0$  and no phase shift occurs. In general, the phase  $\phi_X$  is in the interval  $(-\phi_X^{max} \div \phi_X^{max})$ , where  $\sin \phi_X^{max} = k \tan^2 \theta_{12}$ . This maximal phase corresponds to  $r_X = r\sqrt{1 - k^2 \tan^4 \theta_{12}}$ .

For the elements of  $e$ -row, the  $s_{13}$  corrections should be taken into account (see (A.7)):

$$\begin{aligned} \tilde{m}_{e\mu} &\approx |c_{23}ry + s_{13}s_{23}e^{i(\delta-2\sigma_Y)}|, \\ \tilde{m}_{e\tau} &\approx |s_{23}ry - s_{13}c_{23}e^{i(\delta-2\sigma_Y)}|. \end{aligned} \quad (32)$$



Again, the effect of  $m_1$  is reduced to renormalization of  $r$  and a shift of phase (compare with Eqs.(16,17)):

$$r \rightarrow r_Y \equiv r \frac{y}{s_{12}c_{12}}, \quad \sigma \rightarrow \sigma_Y \equiv \sigma + \frac{1}{2}\phi_Y. \quad (33)$$

Minimal and maximal values of  $r_Y$  are given by:

$$r_Y = \begin{cases} r(1-k), & \text{for } \rho = 0 \\ r(1+k), & \text{for } \rho = \pi/2 \end{cases}.$$

In these extreme cases there is no phase shift. In general, for arbitrary values of  $\rho$ ,  $\phi_Y$  is in the interval  $(-\phi_Y^{max} \div \phi_Y^{max})$ , where  $\sin \phi_Y^{max} = k$  and this maximal value corresponds to  $r_Y = r\sqrt{1-k^2}$ .

Notice that, for  $m_{e\mu}$  and  $m_{e\tau}$ , modifications of  $r$  can be larger than for the elements of  $\mu\tau$ -block; moreover,  $r_Y$  and  $r_X$  are changing with  $\rho$  in opposite phases:  $r_Y$  is minimal when  $r_X$  is maximal or *vice versa*. The phases of variations of  $\mu\tau$ -block elements are correlated as in the hierarchical case. No phase shift among these elements is induced by  $m_1$  contribution: in (21) one should substitute  $\sigma \rightarrow \sigma_X$ . Similar conclusion is valid for  $e$ -row elements: in (22)  $\sigma$  should be substituted by  $\sigma_Y$ .

For the  $ee$ -element, similarly to the previous cases, we get (including  $s_{13}$  corrections):

$$\tilde{m}_{ee} = |c_{13}^2 s_{12}^2 r_Z + s_{13}^2 e^{2i(\delta-\sigma_Z)}|, \quad (34)$$

where

$$r_Z \equiv r \frac{z}{s_{12}^2}, \quad \sigma_Z \equiv \sigma + \frac{1}{2}\phi_Z. \quad (35)$$

Now the difference between  $r$  and  $r_Z$  can be substantially larger:

$$r_Z = \begin{cases} r(1+k \cot^2 \theta_{12}), & \text{for } \rho = 0 \\ r|1-k \cot^2 \theta_{12}|, & \text{for } \rho = \pi/2 \end{cases},$$

and  $r_Z$  changes with  $\rho$  in phase with  $r_X$ . Notice that, for  $k < \tan^2 \theta_{12}$ , the shift  $\phi_Z$  is restricted to the interval  $(-\phi_Z^{max} \div \phi_Z^{max})$ , where  $\sin \phi_Z^{max} = k \cot^2 \theta_{12}$ . For  $k > \tan^2 \theta_{12}$ , the shift is unrestricted. The  $ee$ -element is zero for

$$\tan \theta_{13} = \sqrt{r_Z} = s_{12} \sqrt{r_Z}, \quad \delta - \sigma_Z = \frac{\pi}{2}, \frac{3\pi}{2}.$$

Since  $r_Z$  can be smaller than  $r$ , or even zero, the equality  $m_{ee} = 0$  can be realized for requires smaller values of  $s_{13}$  than in the hierarchical case. Now the strongly hierarchical structure of the  $e$ -row,

$$m_{ee} \ll m_{e\mu} \ll m_{e\tau},$$

can be easily achieved. Maximal value of  $m_{ee}$  equals approximately  $\tilde{m}_{ee}^{max} \approx r(s_{12}^2 + kc_{12}^2)$ .

The dependences of the mass matrix elements on phases can be deduced from Fig.2 and Fig.3. Since, now, the “effective” value of  $r$  is different for the  $\mu\tau$ -block elements ( $r_X$ ) and the  $e$ -row elements ( $r_Y, r_Z$ ), one should take, *e.g.*, lines which correspond to the  $\mu\tau$ -block from Fig.2 and lines which correspond to the  $e$ -row from Fig.3 or *vice versa*.

Let us analyze the dependence of the elements on the phase  $\rho$ . The relative amplitudes of variations of the  $\mu\tau$ -block elements are suppressed by a factor  $s_{12}^2rk$  (see (A.9)):

$$\frac{\Delta m^\rho}{m} \approx s_{12}^2rk \times \begin{cases} \cot^2 \theta_{23}, & m_{\mu\mu} \\ \tan^2 \theta_{23}, & m_{\tau\tau} \\ 1, & m_{\mu\tau} \end{cases} . \quad (36)$$

The influence of  $\rho$  on the  $e$ -row elements is much stronger. For very small  $s_{13}$ , we have

$$m_{e\mu} \approx c_{23}s_{12}c_{12}r|1 - ke^{-2i\rho}|$$

(for  $m_{e\tau}$  one should substitute  $c_{23} \rightarrow s_{23}$ ) and the relative amplitude of variations is given by  $k$ . For the  $ee$ -element the amplitude can be maximal if  $k \geq \tan^2 \theta_{12}$ .

## 4.2 Partial degeneracy

For  $\sqrt{\Delta m_{sol}^2} \ll m_1 \lesssim \sqrt{\Delta m_{atm}^2}$ , we get the spectrum with partial degeneracy  $m_1 \approx m_2 \lesssim m_3$ . The ratios of masses are

$$r \approx \frac{m_1}{\sqrt{m_1^2 + \Delta m_{atm}^2}} \lesssim 1, \quad k \approx 1 - \frac{\Delta m_{sol}^2}{2m_1^2} . \quad (37)$$

For  $m_1 > 2 \cdot 10^{-2}$  eV, the deviation of  $k$  from 1 is smaller than 5% and we can neglect it in comparison with other corrections (related to possible large deviations from maximal 2-3 mixing, and  $s_{13} \gtrsim 0.1$ ). Now the scale of masses is determined by  $m_3 \approx \sqrt{m_1^2 + \Delta m_{atm}^2} \sim (1 \div 2)\sqrt{\Delta m_{atm}^2}$ . The sum of all the matrix elements squared equals

$$S_0 \approx m_3^2(1 + 2r^2) .$$

Let us consider first the dependence of the masses on phase  $\sigma$  (see Figs.4,5 panels a,c,e and phase diagrams in Fig.1). In the limit of small  $s_{13}$ , we get

$$\begin{aligned} \tilde{m}_{\mu\mu} &\approx |s_{23}^2 e^{-2i\sigma} + rc_{23}^2 X_1(\rho)| , \\ \tilde{m}_{\tau\tau} &\approx |c_{23}^2 e^{-2i\sigma} + rs_{23}^2 X_1(\rho)| , \\ \tilde{m}_{\mu\tau} &\approx s_{23}c_{23} |e^{-2i\sigma} - rX_1(\rho)| , \end{aligned} \quad (38)$$

where

$$X_1(\rho) \equiv X(k=1) = c_{12}^2 + s_{12}^2 e^{-2i\rho}. \quad (39)$$

The mass  $\tilde{m}_{\mu\mu}$  oscillates with  $\sigma$  around  $s_{23}^2$ ; the amplitude of variations depends on the phase  $\rho$ . Maximal amplitude is for  $\rho = 0$ , which corresponds to  $X_1 = 1$ . Similarly, the mass  $\tilde{m}_{\tau\tau}$  oscillates in phase with  $\tilde{m}_{\mu\mu}$  around the average value  $c_{23}^2$ . The mass  $\tilde{m}_{\mu\tau}$  varies in opposite phase (due to the minus sign in Eq. (38)). The amplitude of variations of all  $\mu\tau$ -block elements decreases with increase of the phase  $\rho$  and it is minimal for  $\rho = \pi/2$ .

The corrections of order  $s_{13}$  change the amplitudes of variations and produce a phase shift. The largest influence of these corrections is for  $\rho = \pi/2$ . From (A.9) we find

$$\begin{aligned} \tilde{m}_{\mu\mu} &\approx |s_{23}^2 e^{-2i\sigma} + r c_{23}^2 (\cos 2\theta_{12} - 2\epsilon_{\mu\mu})|, \\ \tilde{m}_{\tau\tau} &\approx |c_{23}^2 e^{-2i\sigma} + r s_{23}^2 (\cos 2\theta_{12} + 2\epsilon_{\tau\tau})|, \\ \tilde{m}_{\mu\tau} &\approx s_{23} c_{23} |e^{-2i\sigma} - r (\cos 2\theta_{12} + 2\epsilon_{\mu\tau})|. \end{aligned} \quad (40)$$

For  $\delta = 0$  ( $\epsilon > 0$ ), the corrections suppress the amplitude of variations of  $\tilde{m}_{\mu\mu}$  and enhance the amplitude of  $\tilde{m}_{\tau\tau}$  and  $\tilde{m}_{\mu\tau}$  variations (see Fig.4e). For  $\delta = \pi/2$  ( $\epsilon < 0$ ) the situation is opposite:  $\tilde{m}_{\mu\mu}$  variations are enhanced.

In the approximation (38), all the elements of  $\mu\tau$ -block depend on the phase  $\rho$  in the same way. So, there is no relative shift and the relative phases are determined as in (21). The phase shift seen in Fig.4c is due to the interplay of  $\epsilon$  corrections and phase  $\rho$ .

The dependence of elements of the  $e$ -row on  $\sigma$  (as well as  $\delta$ ) appears due to terms of the order  $s_{13}$  (see (A.11) and Fig.4 panels a,c,e). Neglecting corrections  $\sim r s_{13}$ , we get (for  $\rho$  being not too close to 0):

$$\tilde{m}_{e\mu} \approx |r c_{23} Y_1(\rho) + s_{13} s_{23} e^{i(\delta-2\sigma)}|, \quad \tilde{m}_{e\tau} \approx |r s_{23} Y_1(\rho) - s_{13} c_{23} e^{i(\delta-2\sigma)}|, \quad (41)$$

where

$$Y_1(\rho) \equiv Y(k=1) = s_{12} c_{12} (1 - e^{-2i\rho}). \quad (42)$$

The masses  $\tilde{m}_{e\mu}$  and  $\tilde{m}_{e\tau}$  vary with  $(\delta - 2\sigma)$  in opposite phase (small phase shift may appear due to interplay of order  $r s_{13}$  corrections and phase  $\rho$ ). The amplitude of variations is proportional to  $s_{13}$ . The average values of the elements increase with  $\rho$ , and they reach maxima,  $\tilde{m}_{e\mu}^{max} = r \sin 2\theta_{12} c_{23}$  and  $\tilde{m}_{e\tau}^{max} = r \sin 2\theta_{12} s_{23}$ , at  $\rho = \pi/2$ .

Configuration with  $\rho = 0$  or  $\rho$  close to zero is the special one (see Fig.4a). In this case the main terms in (A.11) vanish and dependence on phases appears due to  $\epsilon$  terms, defined

in (A.12):

$$\begin{aligned}\tilde{m}_{e\mu} &\approx \left| \frac{1}{2}r \sin 2\theta_{12}c_{23} (\epsilon_{e\mu} + \epsilon'_{e\mu}) - s_{13}s_{23}e^{i(\delta-2\sigma)} \right| , \\ \tilde{m}_{e\tau} &\approx \left| \frac{1}{2}r \sin 2\theta_{12}s_{23} (\epsilon_{e\tau} + \epsilon'_{e\tau}) - s_{13}c_{23}e^{i(\delta-2\sigma)} \right| .\end{aligned}\quad (43)$$

Notice that elements  $\tilde{m}_{e\mu}$  and  $\tilde{m}_{e\tau}$  vary in phase; both the average value and the amplitude are proportional to  $s_{13}$ .

Changing the phase  $\delta$  by  $\Delta\delta$  one shifts lines which correspond to the  $e$ -row elements,  $\tilde{m}_{e\mu}$  and  $\tilde{m}_{e\tau}$ , with respect to lines of  $\mu\tau$ -block elements by  $\Delta\sigma = \Delta\delta/2$ . For instance, according to Fig.4c, one can get equalities  $\tilde{m}_{\mu\mu} = \tilde{m}_{\tau\tau} = \tilde{m}_{\mu\tau}$  and  $\tilde{m}_{e\mu} = \tilde{m}_{e\tau}$  simultaneously.

Variations of the  $ee$ -element (A.13) with  $\sigma$  as well as with  $\delta$  are strongly suppressed by the factor  $s_{13}^2$ , so that

$$\tilde{m}_{ee} \approx r |Z_1(\rho)|, \quad (44)$$

where

$$Z_1(\rho) \equiv Z(k=1) = s_{12}^2 + c_{12}^2 e^{-2i\rho}. \quad (45)$$

The average value decreases with increase of the phase  $\rho$ . It varies from  $\tilde{m}_{ee}^{max} \approx r$  for  $\rho \approx 0, \pi$  down to  $\tilde{m}_{ee}^{min} \approx r \cos 2\theta_{12}$  for  $\rho \approx \pi/2$ . Variations of  $\tilde{m}_{ee}$  with  $\rho$  are in opposite phase with respect to  $\tilde{m}_{e\mu}$  and  $\tilde{m}_{e\tau}$ .

Let us analyze the dependence on the phase  $\rho$  (Fig.5 panels a,c,e). The amplitudes of variations of the  $\mu\tau$ -block elements with  $\rho$ ,  $\Delta m^\rho \propto r s_{12}^2$ , are smaller (for non-maximal solar mixing) than the amplitudes of  $\sigma$  variations. The average values of  $\tilde{m}_{\mu\mu}$  and  $\tilde{m}_{\tau\tau}$  decrease whereas the average of  $\tilde{m}_{\mu\tau}$  increases with increase of  $\sigma$  from 0 to  $\pi/2$ . Rather strong split of masses in the  $\mu\tau$ -block (see Fig.5a,5e) is due to cancellation of contributions related to  $m_3$  (first term in (38)) and to  $m_1$  and  $m_2$  (second term). For large  $s_{13}$ , the terms of order  $r s_{13}$  can enhance variations with  $\rho$ .

According to (41), variations of the  $e$ -row elements are strong: the amplitude can be close to maximal. For large values of  $s_{13}$ , the dependence of  $m_{e\mu}$  and  $m_{e\tau}$  on the phase  $(2\sigma - \delta)$  changes significantly the average values of the elements and also modifies the amplitudes of variations.

The matrix elements are all correlated. This can be seen in the limit of very small  $s_{13}$ . For partially degenerate spectrum ( $k=1$ ), we get:

$$\begin{aligned}x = z &= \sqrt{1 - \sin^2 2\theta_{12} \sin^2 \rho}, \\ y &= \sin 2\theta_{12} \sin \rho,\end{aligned}\quad (46)$$

so that  $y = \sqrt{1 - x^2}$ . Moreover,

$$\tan \phi_X = -\frac{\sin 2\rho}{\cot^2 \theta_{12} + \cos 2\rho}. \quad (47)$$

The mass matrix can be written as

$$\tilde{m} = \begin{pmatrix} rx & c_{23}r\sqrt{1-x^2} & s_{23}r\sqrt{1-x^2} \\ \dots & |c_{23}^2rx + s_{23}^2e^{-2i\sigma x}| & s_{23}c_{23}|-rx + e^{-2i\sigma x}| \\ \dots & \dots & |s_{23}^2rx + c_{23}^2e^{-2i\sigma x}| \end{pmatrix}. \quad (48)$$

From (48), we get immediately the following relations among the elements:

$$\tilde{m}_{ee}^2 + \tilde{m}_{e\mu}^2 + \tilde{m}_{e\tau}^2 = r^2; \quad (49)$$

$$\frac{m_{e\mu}}{m_{e\tau}} = \tan \theta_{23}; \quad (50)$$

$$\tilde{m}_{\tau\tau}^2 - \tilde{m}_{\mu\mu}^2 = (1 - r^2x^2) \cos 2\theta_{23}. \quad (51)$$

Notice that  $m_{\tau\tau} = m_{\mu\mu}$  either for  $\theta_{23} = 45^\circ$  or for  $rx = 1$ . The latter corresponds to completely degenerate spectrum and  $\rho = 0$ . In this case

$$\tilde{m}_{\tau\tau} = \tilde{m}_{\mu\mu} = \sqrt{1 - \sin^2 2\theta_{23} \sin^2 \sigma}, \quad \tilde{m}_{\mu\tau} = \sin 2\theta_{23} \sin \sigma.$$

Furthermore, we find, for the sum of the  $\mu\tau$ -block elements,

$$\tilde{m}_{\mu\mu}^2 + \tilde{m}_{\tau\tau}^2 + 2\tilde{m}_{\mu\tau}^2 = 1 + r^2x^2$$

and consequently:

$$\tilde{m}_{\mu\mu}^2 + \tilde{m}_{\tau\tau}^2 + 2\tilde{m}_{\mu\tau}^2 - \tilde{m}_{ee}^2 = 1.$$

For a given  $r$  the mass matrix (48) is determined by  $\sigma_X$  and  $x$ . In general  $\sigma_X$  and  $x$  can be treated as two independent parameters. Depending on  $\rho$ ,  $x$  changes from the minimal value  $x^{\min} \equiv \cos 2\theta_{12}$ , for  $\rho = \pi/2$ , to  $x^{\max} \equiv 1$ , for  $\rho = 0$ . The phase  $\phi_X$  varies in a rather narrow interval, which decreases with  $\theta_{12}$ :

$$\sin \phi_X \sim (-\tan^2 \theta_{12} \div \tan^2 \theta_{12}).$$

### 4.3 Degenerate spectrum

For  $m_1 \gg \sqrt{\Delta m_{atm}^2}$ , we have  $m_1 \approx m_2 \approx m_3$ , and the ratio of masses is given by

$$r \approx 1 - \frac{\Delta m_{atm}^2}{2m_1^2}.$$

For  $m_1 = 0.5$  eV, the deviation of  $r$  from 1 is smaller than 1% and we can neglect it in comparison with other small parameters,  $s_{13}$  and  $\xi$ . The  $e$ -row elements and the  $\mu\tau$ -block elements are given by (A.9,A.11,A.13), with  $k = r = 1$ . Notice that, in the approximation  $\Delta m_{atm}^2 \approx 0$ , the structure of the mass matrix for normal and inverted hierarchy is the same.

Transition to the degeneracy case does not produce qualitative changes in dependences of the matrix elements on phases in comparison with partial degeneracy case (see Fig.4 b,d,f and Fig.5 b,d,f). Amplitudes of variations of the  $\mu\tau$ -block elements increase and can reach maximal size for specific values of phases. This leads to zero (small) values of certain matrix elements and therefore to the appearance of a hierarchical structure of the mass matrix. For example, in the case of maximal 2-3 mixing and  $\rho = 0$ , we find from (48):

$$\tilde{m} \approx \begin{pmatrix} 1 & 0 & 0 \\ \dots & \frac{1}{2}|1 + e^{-2i\sigma}| & \frac{1}{2}|-1 + e^{-2i\sigma}| \\ \dots & \dots & \frac{1}{2}|1 + e^{-2i\sigma}| \end{pmatrix}. \quad (52)$$

Therefore,  $\tilde{m}_{\mu\mu} = \tilde{m}_{\tau\tau} = 0$  for  $\sigma = \pi/2$  (Fig.4b). Moreover,  $\epsilon$  corrections cancel in (A.9), for  $k = 1$  and  $\rho = 0$ . For non-maximal 2-3 mixing, using (38) we find that  $\tilde{m}_{\mu\mu} = 0$  for

$$\sin^2 \rho = \frac{\cos 2\theta_{23}}{c_{23}^4 \sin^2 2\theta_{12}}, \quad \cos 2\sigma = -\frac{c_{23}^4 \cos 2\theta_{12} + s_{23}^4}{2c_{12}^2 s_{23}^2 c_{23}^2}.$$

In this case, however,  $\tilde{m}_{\tau\tau}$  differs from zero. Such a configuration is realized approximately in Fig.4d.

The average values of  $\tilde{m}_{e\mu}$  and  $\tilde{m}_{e\tau}$  increase with respect to the partial degeneracy case, whereas the amplitudes of variations with  $\sigma$  and  $\rho$  do not change. Average value of the  $ee$ -element increases with  $r$  and can reach 1 for  $\rho = 0$  (Fig.4b).

The amplitudes of variations with  $\rho$  (Fig.5 b,d,f) increase and, for  $\rho \approx 0, \pi$ , hierarchical structure of the mass matrix appears (Fig.5b,5f). For some cases all the elements become approximately equal to each other (see, *e.g.*, Fig.5d at  $\rho = 1.3\pi$ ).

## 4.4 From hierarchy to degeneracy

In Fig.6, we show the dependence of  $m_{\alpha\beta}$  on  $m_1$  for different values of the Majorana phases  $\sigma$  and  $\rho$ . As follows from the figure, the hierarchical structure with the dominant  $\mu\tau$ -block and small  $e$ -row elements exists, independently on phases, for  $m_1/\sqrt{\Delta m_{atm}^2} \lesssim 0.1$  ( $m_1 \lesssim 0.005$  eV). This interval of  $m_1$  corresponds to hierarchical or non-degenerate spectra. The structure with dominant  $\mu\tau$ -block disappears for  $m_1/\sqrt{\Delta m_{atm}^2} \sim 0.3 \div 0.5$  ( $m_1 < (0.02 \div 0.03)$  eV), that is for partially degenerate spectrum. For  $m_1 \gtrsim \sqrt{\Delta m_{atm}^2} \approx 0.05$  eV, the spectrum converges to the degenerate one. In this last case, the structure of the mass matrix depends substantially on the Majorana phases. Notice that, in general, the pairs of elements  $\tilde{m}_{\mu\mu}$  and  $\tilde{m}_{\tau\tau}$ , as well as  $\tilde{m}_{e\mu}$  and  $\tilde{m}_{e\tau}$ , have similar dependences on  $m_1$ .

For large part of the phase parameter space, all elements of the mass matrix increase with  $m_1$  being of the same order. Some accidental equalities among them may appear. Particular structures are realized for specific values of phases:  $\rho, \sigma \approx 0, \pi/4, \pi/2$ .

## 5 $\rho - \sigma$ plots and neutrinoless $2\beta$ decay

### 5.1 $\rho - \sigma$ plots

In spite of large freedom related to the unknown CP-phases,  $\sigma$ ,  $\rho$ ,  $\delta$ , scale  $m_1$  and  $s_{13}$ , already the present data give important restrictions on structure of the mass matrix. The dependences of various matrix elements on phases are correlated. These features can be seen in the  $\rho - \sigma$  plots. In Figs.7-13, we show contours of constant values of  $m_{\alpha\beta}$  in the plane of the Majorana phases.

Let us comment on properties of the  $\rho - \sigma$  plots.

The periodicity in  $\rho$  and  $\sigma$  implies that the opposite sides of the plots must be identified. For example, the case of equal CP parities of  $\nu_1$ ,  $\nu_2$  and  $\nu_3$  corresponds to any of the four corners of the plots.

In general, any pair of values  $(\rho, \sigma)$  in the range  $[0, \pi) \times [0, \pi)$  represents a physically independent situation. However, if  $\delta = 0$ , it follows from (4) that

$$m_{\alpha\beta}(\sigma, \rho) = m_{\alpha\beta}(\pi - \sigma, \pi - \rho) .$$

This reflection symmetry is present in Figs.7-9, Figs.11-13, but not in Fig.10, where  $\delta = \pi/2$ .

The phase  $\rho$  is associated with the mass  $m_1$ , therefore, in the case of strong normal hierarchy, the dependence of  $m_{\alpha\beta}$  on  $\rho$  disappears and the iso-mass contours become parallel

to the axis  $\rho$ . In contrast, the contours for  $m_{ee}$  are nearly parallel to  $\sigma$  axis, since  $m_{ee}$  depends on  $\sigma$  via  $O(s_{13}^2)$  terms. There is a relative shift of  $\pi/2$ , along the axis  $\sigma$ , between the patterns for  $m_{e\mu}$  and  $m_{e\tau}$ .

The elements  $m_{\mu\mu}$  and  $m_{\tau\tau}$  have have the same  $\rho - \sigma$  pattern in the limit of maximal 2-3 mixing and zero  $s_{13}$ . The difference between them originates from deviation of  $\theta_{23}$  from  $45^\circ$  and from the terms (see (A.7))

$$\pm \sin 2\theta_{23}s_{13}r e^{-i\delta} Y, \quad (53)$$

where the plus sign corresponds to  $m_{\tau\tau}$  and the minus sign to  $m_{\mu\mu}$ . In the case of maximal 2-3 mixing, only the term (53) contributes to the difference. The pattern for  $m_{\mu\tau}$  is complementary to that for  $m_{\mu\mu}$  and  $m_{\tau\tau}$ , in the sense that regions of large  $m_{\mu\tau}$  correspond to regions of small  $m_{\mu\mu}$  and  $m_{\tau\tau}$  and *vice versa*.

Small values of the  $\mu\tau$ -block elements appear at the corners of the plots,  $\rho \approx 0, \pi$  as well as  $\sigma \approx 0, \pi$ , and in the region  $\sigma \sim \pi/2$ . In the latter case, the corresponding value of  $\rho$  depends on 2-3 mixing. For maximal mixing, the regions of small elements are at  $\rho \sim 0, \pi$ ; with deviation from maximal mixing, the regions shift to the center of the plot and merge at  $\rho \sim \pi/2$  for large values of  $\xi$ .

Let us comment on specific features of Figs.7-13.

In Fig.7 we show the plots for the non-degenerate spectrum. There is a sharp separation of the  $e$ -row and dominant  $\mu\tau$ -block elements. Structuring within these two groups is rather weak.

In Fig.8 we show the plots for spectrum with partial degeneracy. Dependence of elements on  $\rho$  becomes stronger with increase of  $m_1$ . The  $\mu\tau$ -block elements have more profound structure. The elements  $m_{e\mu}$  and  $m_{e\tau}$  have small values in the regions near the corners of the plots.

The plots for spectrum with strong degeneracy are shown in Figs.9-13. Now the  $e$ -row elements depend strongly on  $\rho$ , whereas the dependence on  $\sigma$  is rather weak. With increase of  $m_1$  the  $\rho$ -dependence becomes stronger for  $\mu\tau$ -block elements (see (A.9)). The patterns for  $m_{\mu\mu}$  and  $m_{\tau\tau}$  differ due to order  $s_{13}$  terms (53), which also depend on  $\delta$ . The contribution of the term (53) has minus sign for  $m_{\mu\mu}$  and therefore it adds constructively with the other  $\rho$ -dependent term (see (A.9)). For  $m_{\tau\tau}$ , instead, the contribution has an opposite sign, therefore  $\rho$ -dependence remains weak.

In Fig.10 we show the plots for  $\delta = \pi/2$ . The difference between the plots for  $m_{\mu\mu}$  and  $m_{\tau\tau}$  becomes smaller in comparison with the case  $\delta = 0$ : in fact, for  $\delta = \pi/2$ , the term (53) has pure imaginary coefficient and its contribution to  $m_{\mu\mu}$  and  $m_{\tau\tau}$  becomes similar.



For  $\delta = \pi$ , the  $\rho - \sigma$  plots for  $m_{\mu\mu}$  and  $m_{\tau\tau}$  interchange as compared with those in Fig.9. The element  $m_{\mu\tau}$  is almost unchanged. In the first approximation, the effect of  $\delta = \pi/2$  on the  $e$ -row elements is reduced to a shift of  $\sigma$  by  $\pi/4$  for  $m_{e\mu}$  and  $m_{e\tau}$  and by  $\pi/2$  for  $m_{ee}$ .

In Fig.11 we show the plots for small  $s_{13}$ . With decrease of  $s_{13}$ , dependence of  $e$ -row elements on  $\sigma$  disappears, patterns for  $m_{\mu\mu}$  and  $m_{\tau\tau}$  become more similar, complementarity to that for  $m_{\mu\tau}$  becomes sharp.

In Fig.12 we show the plots for non-maximal 2-3 mixing ( $\theta_{23} = 35^\circ$ ). The pattern for  $m_{ee}$  is unchanged and the one for  $m_{\mu\tau}$  changes weakly. In contrast, the difference between the patterns for  $m_{e\mu}$  and  $m_{e\tau}$  increases. In particular,  $m_{e\mu}$  can be large for  $\rho \approx \pi/2$  and  $\sigma \approx 0, \pi$ . Also difference of the patterns for  $m_{\mu\mu}$  and  $m_{\tau\tau}$  increases. Dependence of  $m_{\tau\tau}$  on phases becomes weaker and regions with very small values of  $m_{\tau\tau}$  disappear. In contrast, for  $m_{\mu\mu}$  the region of small values appears near the center of the plot:  $\rho \sim \sigma \sim \pi/2$ . For  $\theta_{23} > 45^\circ$  (not shown) the situation is opposite: region of small values at  $\rho \sim \sigma \sim \pi/2$  appears for  $m_{\tau\tau}$ . Also  $m_{e\tau}$  becomes, in general, larger than  $m_{e\mu}$ .

In Fig.13 we show the plots for maximal 1-2 mixing. The  $\rho$  dependence becomes strong for all the elements and especially for  $m_{ee}$ . This element can be zero at  $\rho \approx \pi/2$ .

## 5.2 $\beta\beta_{0\nu}$ -decay and structure of the mass matrix

The  $ee$ -element,  $m_{ee}$ , is the only matrix element for which we have immediate experimental access (present bounds on other elements are very far from expected values [20]). The  $\rho - \sigma$  plots allow one to find immediately the implications of the results from  $\beta\beta_{0\nu}$ -decay searches for the structure of the mass matrix (in assumption that the exchange of the light Majorana neutrinos is the only mechanism of the decay). For  $m_{ee}$ , the Majorana phase plots (defined differently from  $\rho$  and  $\sigma$  have been considered in [31]).

The iso-mass contours of  $m_{ee}$  are nearly parallel to the axis  $\sigma$ . Weak dependence of  $m_{ee}$  on  $\sigma$  appears due to term of the order  $s_{13}^2$ . For very small  $s_{13}$  and (partially) degenerate spectrum, the iso-mass contours are determined by

$$m_{ee} = m_1 \sqrt{1 - \sin^2 2\theta_{12} \sin^2 \rho}. \quad (54)$$

Suppose that experimental searches give the upper bound  $m_{ee} < m_{ee}^{up}$ . There are two iso-mass contours which correspond to a given value  $m_{ee}^{up}$ . For negligible  $s_{13}$ , they are at some  $\rho^{up} < \pi/2$  and at  $\pi - \rho^{up}$ . We will denote these contours, respectively,  $m_{ee}^L(\rho, \sigma, m_1, \theta_{12}, s_{13})$  and  $m_{ee}^R(\rho, \sigma, m_1, \theta_{12}, s_{13})$ . The upper experimental limit on  $m_{ee}$  excludes the following regions in the  $\rho - \sigma$  plots (obviously for all the matrix elements):

- the region between the left border of the panel,  $\rho = 0$ , and the iso-mass contour  $m_{ee}^L$ ;
- the region between the iso-mass contour  $m_{ee}^R$  and the right border at  $\rho = \pi$ .

The position and the shape of contours depend on  $m_1$ ,  $\theta_{12}$  and  $s_{13}$ . Taking, *e.g.*,  $m_1 = 0.5$  eV,  $s_{13} = 0.1$ ,  $\tan^2 \theta_{12} = 0.36$  and the bound (10), we find from Fig.9 that the regions covered by the three darkest strips are excluded. They correspond approximately to  $\rho < \pi/4$  and  $\rho > 3\pi/4$ . These regions are excluded for all the elements. So, in this particular case, all corners of the plots and sides with  $\rho \approx 0, \pi$ , which correspond to hierarchical structure of the mass matrix, are excluded. Clearly no constraint on the structure appears for weaker bound,  $m_{ee}^{up} > 0.5$  eV (which is allowed by the uncertainty in the nuclear matrix elements), or for  $m_1 < m_{ee}^{up}$ .

For small  $s_{13}$ , the mass matrix can be written immediately in terms of  $m_{ee}$ , using Eq.(48):

$$\tilde{m} = \begin{pmatrix} \tilde{m}_{ee} & c_{23}\sqrt{r^2 - \tilde{m}_{ee}^2} & s_{23}\sqrt{r^2 - \tilde{m}_{ee}^2} \\ \dots & |c_{23}^2\tilde{m}_{ee} + s_{23}^2e^{-2i\sigma x}| & |s_{23}c_{23} - \tilde{m}_{ee} + e^{-2i\sigma x}| \\ \dots & \dots & |s_{23}^2\tilde{m}_{ee} + c_{23}^2e^{-2i\sigma x}| \end{pmatrix}. \quad (55)$$

Here  $\tilde{m}_{ee} = xr \leq r$ . This form shows how strongly the determination of  $\tilde{m}_{ee}$  can influence the structure of the mass matrix. Large values of  $s_{13}$  give corrections to (55), which can weakly modify the structure of the matrix.

Positive results of  $\beta\beta_{0\nu}$ -decay searches will select two strips in the  $\rho - \sigma$  plot.

Substantial bounds on the structure of the mass matrix can be obtained when future solar neutrino experiments and KamLAND [24] experiment will stronger restrict the allowed range for  $\theta_{12}$  and also when future  $\beta$  decay measurements (KATRIN [32]) will strengthen the bound on the absolute mass scale.

## 6 CP phases and structure of the mass matrix

Possible structures of the mass matrix can be classified in the following way:

1. Hierarchical matrices, with certain dominant and sub-dominant elements.
2. Matrices with certain ordering of elements. In this case, the elements  $m_{\alpha\beta}$  have the same order of magnitude, but still there are inequalities, which are correlated with the flavor of neutrinos.
3. Democratic matrices, with equal moduli of all the elements:  $m_{\alpha\beta} \approx m_0$  for any choice of  $\alpha, \beta$ .

#### 4. Matrices without flavor alignment (flavor “anarchy”).

We will discuss these possibilities in order.

### 6.1 Hierarchical mass matrices

The regions of parameters which correspond to a hierarchical structure of the mass matrix can be identified as “white” zones in  $\rho - \sigma$  plots, where one or several elements have small values.

A systematic search of possible hierarchical structures can be performed in the following way. In the limit  $s_{13} = 0$ , the elements of  $e$ -row equals:

$$\tilde{M}_{e\tau} = -\tan\theta_{23}\tilde{M}_{e\mu} = -rs_{23}Y = -rs_{23}s_{12}c_{12}(1 - ke^{-2i\rho}) . \quad (56)$$

Since  $\tan\theta_{23} \sim 0.7 - 1.4$ , these elements can be either both small or both large.

Let us consider first the case when  $m_{e\mu}$  and  $m_{e\tau}$  do not belong to the dominant structure, *i.e.*,  $\tilde{M}_{e\mu} \approx \tilde{M}_{e\tau} \approx 0$ . According to (56), this implies either  $r \rightarrow 0$  or  $\rho \approx 0, \pi$ . In the first case we arrive at the structure with dominant  $\mu\tau$ -block:

$$\tilde{M} = e^{-2i\sigma} \begin{pmatrix} 0 & 0 & 0 \\ \dots & s_{23}^2 & s_{23}c_{23} \\ \dots & \dots & c_{23}^2 \end{pmatrix} + \mathcal{O}(s_{13}, r) , \quad (57)$$

which holds for any value of the phases (see Fig.7). Weak ordering of elements is possible in the  $\mu\tau$ -block. In the second case,  $\rho = 0, \pi$ , which corresponds to the same CP-parity of  $\nu_1$  and  $\nu_2$ , the ratio  $r$  can be of order 1 and new structures appear. For  $\rho = 0, \pi$ , we get  $X = Z = 1$  and (see (48)):

$$\tilde{M} = \begin{pmatrix} r & 0 & 0 \\ \dots & c_{23}^2 r + s_{23}^2 e^{-2i\sigma} & s_{23}c_{23}(-r + e^{-2i\sigma}) \\ \dots & \dots & s_{23}^2 r + c_{23}^2 e^{-2i\sigma} \end{pmatrix} + \mathcal{O}(s_{13}) . \quad (58)$$

Such a possibility is realized near the left and right borders of the plots in Fig.8. The determinant of the  $\mu\tau$ -block is given by

$$\tilde{M}_{\tau\tau}\tilde{M}_{\mu\mu} - \tilde{M}_{\mu\tau}^2 \approx re^{-2i\sigma} .$$

So, with increase of  $r$ , it strongly deviates from zero. In the first approximation, we get mass matrix with 4 independent dominant elements of the same order:  $m_{ee} \sim m_{\mu\mu} \sim m_{\tau\tau} \sim m_{\mu\tau}$ .

Hierarchy of elements in the  $\mu\tau$ -block appears for special values of the phase  $\sigma$ . If, *e.g.*,  $\tan\theta_{23} \leq 1$ , we can get  $M_{\mu\mu} \approx 0$  provided that

$$\sigma = \frac{\pi}{2}, \quad r = \tan^2\theta_{23}.$$

The mass matrix is then reduced to

$$\tilde{M} \approx \begin{pmatrix} \tan^2\theta_{23} & 0 & 0 \\ \dots & 0 & -\tan\theta_{23} \\ \dots & \dots & -1 + \tan^2\theta_{23} \end{pmatrix} = \begin{pmatrix} r & 0 & 0 \\ \dots & 0 & -\sqrt{r} \\ \dots & \dots & -1 + r \end{pmatrix}. \quad (59)$$

Let us underline that such a structure is present in the case of partial degeneracy only.

In the limit of complete degeneracy,  $r \rightarrow 1$ , the condition  $M_{\mu\mu} \approx 0$  requires  $\tan\theta_{23} = 1$  and therefore the matrix converges to

$$\tilde{m} = \begin{pmatrix} 1 & \mathcal{O}(s_{13}) & \mathcal{O}(s_{13}) \\ \dots & \mathcal{O}(s_{13}^2) & 1 \\ \dots & \dots & \mathcal{O}(s_{13}^2) \end{pmatrix}. \quad (60)$$

This type of matrix has been discussed previously, *e.g.* in [6]. If also  $\delta = \pi/2$ , then  $Z' = 0$  (see (A.8)) and therefore order  $s_{13}$  terms are zero (see (A.7) and Fig.10).

If  $\tan\theta_{23} \geq 1$ , one can get  $M_{\tau\tau} \approx 0$ . This, again, requires  $\sigma = \pi/2$  but  $r = \cot^2\theta_{23}$  and, in lowest order in  $s_{13}$ , the mass matrix has the form

$$\tilde{M} \approx \begin{pmatrix} \cot^2\theta_{23} & 0 & 0 \\ \dots & -1 + \cot^2\theta_{23} & -\cot\theta_{23} \\ \dots & \dots & 0 \end{pmatrix} = \begin{pmatrix} r & 0 & 0 \\ \dots & -1 + r & -\sqrt{r} \\ \dots & \dots & 0 \end{pmatrix}. \quad (61)$$

It has the same limit (60) in the case of completely degenerate spectrum.

Notice that in the limit  $s_{13} \rightarrow 0$ , one should take into account the deviations of  $k$  from 1. This leads to appearance of terms of order  $\Delta m_{sun}^2/2m_1^2$  instead of zeros (see (37)).

According to (58), the off-diagonal elements of  $\mu\tau$ -block are zero for  $r = e^{-2i\sigma}$ , that is for  $r = 1$  and  $\sigma = 0, \pi$ . In this case  $\tilde{M}_{ee} = \tilde{M}_{\mu\mu} = \tilde{M}_{\tau\tau} = 1$  and

$$\tilde{m} = \begin{pmatrix} 1 & \mathcal{O}(s_{13}) & \mathcal{O}(s_{13}) \\ \dots & 1 & \mathcal{O}(s_{13}^2) \\ \dots & \dots & 1 \end{pmatrix}. \quad (62)$$

So, the dominant structure reduces to the unit matrix (as it has been described, *e.g.*, in [6]) with small off-diagonal corrections (Fig.6a). If also  $\delta = 0, \pi$ , the order  $s_{13}$  terms are zero (see (A.7,A.8)).

Let us study possible equalities of elements of the dominant structure. The conditions for the equality  $m_{\mu\mu} = m_{\tau\tau}$  follow from Eq.(51). All the elements of  $\mu\tau$ -block have the same absolute value provided that 2-3 mixing is maximal and  $\sigma = \pi/4, 3\pi/4$ . In this case:

$$\tilde{M} = \begin{pmatrix} r & 0 & 0 \\ \dots & \frac{1}{2}\sqrt{1+r^2}e^{\pm\phi} & \frac{1}{2}\sqrt{1+r^2}e^{\mp\phi} \\ \dots & \dots & \frac{1}{2}\sqrt{1+r^2}e^{\pm\phi} \end{pmatrix} + \mathcal{O}(s_{13}), \quad (63)$$

where  $\phi = \arctan 1/r$ .

For  $r = 1$ , we get:

$$\tilde{m} = \begin{pmatrix} 1 & \mathcal{O}(s_{13}) & \mathcal{O}(s_{13}) \\ \dots & 1/\sqrt{2} & 1/\sqrt{2} \\ \dots & \dots & 1/\sqrt{2} \end{pmatrix}. \quad (64)$$

Order  $s_{13}$  terms are zero if also  $\delta = \sigma$  or  $\sigma + \pi$ .

Notice that mass matrices considered above depend on  $r$  and  $s_{23}$ . Dependence on  $\theta_{12}$  appears only via  $s_{13}$  and  $\Delta m_{sun}^2/m_1^2$  corrections.

Let us consider the case where  $M_{e\mu}$  and  $M_{e\tau}$  belong to the dominant structure. According to (56), this implies  $r \sim 1$  and  $\rho$  not too close to  $0, \pi$  (see regions with  $\rho \sim \pi/2$  in Figs.9-13). In this case, also the element  $m_{ee}$  can belong to the dominant structure. Indeed, minimal value of  $m_{ee}$  is achieved at  $\rho = \pi/2$ , so that:

$$\frac{m_{ee}^{min}}{m_{e\mu}} = \frac{m_{ee}^{min}}{\tan \theta_{23} m_{e\tau}} = \frac{\cos 2\theta_{12}}{c_{23} \sin 2\theta_{12}}. \quad (65)$$

So, all the elements of  $e$ -row have comparable values, unless 1-2 mixing is near maximal. For  $\theta_{12} \approx \pi/4$ , the hierarchical structure  $m_{ee} \ll m_{e\mu}, m_{e\tau}$  is realized (see Fig.13).

Let us consider the possibility of zeros in the  $\mu\tau$ -block. Now the situation differs from that of the case  $\rho = 0, \pi$  (see Eqs.(46,48)). Since  $x < 1$ , we have  $\tilde{m}_{\mu\tau} \neq 0$  and for maximal mixing, all elements of the  $\mu\tau$ -block differ from zero. Still, for non maximal 2-3 mixing, we can get  $\tilde{m}_{\mu\mu} = 0$  or  $\tilde{m}_{\tau\tau} = 0$ . For instance, if  $\theta_{23} < 45^\circ$ ,  $\tilde{m}_{\mu\mu} = 0$  when  $\sigma_X = \pi/2$  and  $\tan^2 \theta_{23} = xr$ . So, in the case of large  $e$ -row elements, one or two of the diagonal elements can be zero:  $m_{ee}$ , for maximal 1-2 mixing and/or  $m_{\mu\mu}$  ( $m_{\tau\tau}$ ), for special relation among  $\theta_{12}, \sigma$  and  $\theta_{23}$ .

## 6.2 Mass matrices with specific ordering of elements

For  $m_1 \gtrsim \sqrt{\Delta m_{atm}^2}$  ( $k \approx 1$ ), in large part of the phases space, all the elements of the mass matrix are of the same order (see Figs.9-13). Parameters can be found in such a way that

any element of the matrix can be the smallest one or the largest one. Also one can reach equalities between some of the elements. A number of configurations is possible, with only a few restrictions determined by relations among the elements, discussed at the end of section 4.2.

In this connection, let us consider the possibility that masses decrease with transition from the  $\tau$ -flavor to the  $e$ -flavor, that is,

$$m_{\tau\tau} \gtrsim m_{\mu\tau} \gtrsim m_{\mu\mu} \gtrsim m_{e\tau} \gtrsim m_{e\mu} \gtrsim m_{ee} . \quad (66)$$

We will call this possibility the *flavor ordering*. The ordering with  $m_{e\tau} \lesssim m_{\mu\mu}$  is also possible. Notice that, according to (51),  $m_{\tau\tau} > m_{\mu\mu}$  provided that  $\theta_{23} < 45^\circ$ . In contrast, one gets from (50) that  $m_{e\tau} > m_{e\mu}$ , if  $\theta_{23} > 45^\circ$ . So, in the approximation  $s_{13} \approx 0$ , the “flavor ordering” is impossible. However, for near maximal 2-3 mixing, the differences  $m_{\tau\tau} - m_{\mu\mu}$  and  $m_{e\tau} - m_{e\mu}$  are so small that corrections due to non-zero  $s_{13}$  become important (see, in particular, (B.4,B.5)). The  $s_{13}$  corrections can produce flavor ordering, as can be seen, *e.g.*, in Fig.3b, for the case  $m_1 = 0$  and in Fig.4e (shifting  $e$ -row lines), for the case  $r \sim 1$ .

Varying  $r$ ,  $x$ ,  $\sigma_X$  and  $\theta_{23}$  (see (48)), one can get equalities among various elements of the matrix. In particular,

- 1)  $m_{ee} = m_{e\mu}$  for

$$x = \frac{c_{23}}{\sqrt{1 + c_{23}^2}} .$$

- 2)  $m_{ee} = m_{e\tau}$  for  $x$  given by a similar expression with the substitution  $c_{23} \leftrightarrow s_{23}$ .

- 3) All elements of the  $e$ -row are equal for maximal 2-3 mixing and  $x = 1/\sqrt{3}$ .

- 4) One can reach equality of the diagonal elements  $m_{ee} = m_{\mu\mu}$  or  $m_{ee} = m_{\tau\tau}$  and also  $m_{ee} = m_{\mu\mu} = m_{\tau\tau}$ ; see, *e.g.*, Fig.4c.

- 5) The equality of elements of the second diagonal,  $m_{e\tau} = m_{\mu\mu} = m_{\tau e}$ , is possible, but in this case other elements are not small:  $m_{\tau\tau} \approx m_{\mu\mu}$ , for example.

- 6) According to Fig.4d the following relation is possible

$$m_{ee} = m_{\mu\mu} = m_{\tau\tau} \approx 2m_{e\mu} = 2m_{e\tau} = 2m_{\mu\tau}$$

for  $\sigma \approx 0.7$ .

- 7) For  $\sigma \approx 1.2$  (Fig.4d) we find

$$m_{ee} = m_{\mu\tau} \approx 2m_{\tau\tau} = 2m_{e\mu} = 2m_{e\tau} = 2m_{\mu\mu} .$$

However, it is not possible to get zero values of all the diagonal elements. Indeed,  $m_{ee}$  vanishes for  $r = 0$  or  $x = 0$  (the latter corresponds to near maximal 1-2 mixing). However, for  $x = 0$ ,  $m_{\mu\mu}$  and  $m_{\tau\tau}$  are non-zero: they belong to the dominant structure. The only possibility would be to consider inverted hierarchy of the mass eigenvalues.

As follows from the figures 4 - 6, in a number of cases (values of phases) the matrix can show flavor disordering. That is, the relative values of matrix elements can take values between 0 and 1 without correlation with masses of the charge leptons.

### 6.3 Democratic mass matrix

It is possible to have equal absolute values for all the matrix elements in the flavor basis. To obtain such a “democratic matrix” one should satisfy five equalities among independent matrix elements  $m_{\alpha\beta}$ . In general, we have nine parameters (three masses, three mixing angles and three CP violating phases) and we should reproduce the solar as well as atmospheric mass squared differences and mixing angles (4 relations) as well as satisfy the CHOOZ bound. So, in principle, the problem is non-trivial. Let us present one realization of such a possibility.

The  $e$ -row elements should be as large as the  $\mu\tau$ -block elements; this requires  $r \sim 1$  and  $\rho \sim \pi/2$ . The  $\mu\tau$ -block elements are equal to each other only for  $\sigma \sim \pi/4, 3\pi/4$ . Then, if  $s_{13}$  is very small, also  $\xi$  is required to be very small, otherwise  $m_{e\mu}$  is inevitably different from  $m_{e\tau}$  and the same is true for  $m_{\mu\mu}$  and  $m_{\tau\tau}$ .

Taking the limit  $s_{13} = 0, k = 1$  (see (48)), we find from equality of the  $e$ -row elements:

$$\xi = 0, \quad \sin^2 2\theta_{12} \sin^2 \rho = \frac{2}{3}. \quad (67)$$

According to the last equality in (67) the solar mixing angle determines the Majorana phase  $\rho$ . Equality of the  $\mu\tau$ -block elements leads to the condition

$$\cos 2\sigma c_{12}^2 + \cos 2(\sigma - \rho) s_{12}^2 = 0, \quad (68)$$

which fixes the value of  $\sigma$ . If conditions (67) and (68) are satisfied, it turns out that the elements of  $e$ -row and  $\mu\tau$ -block are also equal. Moreover,  $\tilde{m}_{\alpha\beta} = \tilde{m}_0 = 1/\sqrt{3}$ . Notice that last equality can be immediately obtained from the mass squared conservation (section 2.2). Indeed, in the degeneracy case we have  $S_0/m_3^2 \equiv \sum_i \tilde{m}_i^2 = 3$ . For the democratic matrix the sum of all elements equals  $\sum_{\alpha,\beta} \tilde{m}_{\alpha\beta}^2 = 9\tilde{m}_0^2$ . According to the mass conservation, we have  $9\tilde{m}_0^2 = S_0/m_3^2 = 3$ , or  $\tilde{m}_0^2 = 1/3$ .

## 6.4 Bi-maximal mixing and its variations

The Fig.13 corresponds to bi-maximal mixing. Notice that, in contrast with pure bi-maximal mixing,  $\theta_{13}$  is non-zero in the figure. The limit  $\theta_{13} \rightarrow 0$  leads to disappearance of the dependence of  $e$ -row elements on  $\sigma$  and to equality of the patterns for  $m_{\mu\mu}$  and  $m_{\tau\tau}$ .

According to Fig.13, large variety of mass matrix structures can lead to bi-maximal mixing. In particular, for  $\rho = 0, \pi$  and  $\sigma = 0, \pi$  (corners of the plot), we get the nearly diagonal matrix (62). For  $\rho = 0, \pi$  and  $\sigma = \pi/2$ , the mass matrix has the form (60). For  $\rho = \pi/2$ , it follows  $x = 0$ . In this case, for any value of  $\sigma$ , we get the matrix

$$\tilde{m} \approx \frac{1}{2} \begin{pmatrix} 0 & \sqrt{2} & \sqrt{2} \\ \sqrt{2} & 1 & 1 \\ \sqrt{2} & 1 & 1 \end{pmatrix}, \quad (69)$$

discussed in the literature.

Apart of that, many other possibilities are allowed, *e.g.* matrices with nearly equal elements, etc.

## 6.5 Parameterization of $M$

Let us consider the possibility to parameterize the mass matrix by powers of a unique expansion parameter  $\lambda \ll 1$ :

$$\tilde{m}_{\alpha\beta} = c_{\alpha\beta} \lambda^{n_{\alpha\beta}}, \quad (70)$$

where  $c_{\alpha\beta}$  are numbers of order 1. In the flavor symmetry context, the exponents  $n_{\alpha\beta}$  are related to the flavor charges of the corresponding mass terms. If  $n_{\alpha\beta} = n_\alpha + n_\beta$ , where  $n_\alpha$ ,  $n_\beta$  ( $\alpha, \beta = e, \mu, \tau$ ) are numbers associated with corresponding flavor states, factorization occurs:

$$\tilde{m}_{\alpha\beta} = c_{\alpha\beta} \lambda^{n_\alpha} \lambda^{n_\beta}. \quad (71)$$

In this case the smallness of various mass terms is correlated:  $n_{\mu\mu} = 2n_{\mu\tau} - n_{\tau\tau}$ ,  $2n_{e\mu} = n_{ee} + n_{\mu\mu}$ , etc.

Let us first consider the case of spectrum with normal mass hierarchy. As one can see in Eq.(14), for maximal 2-3 mixing and  $\sigma \approx \pi/4, 3\pi/4$ , all elements of the dominant  $\mu\tau$ -block can be equal to each other. Then, the elements of the  $e$ -row should be suppressed by powers of  $\lambda$ :

$$\tilde{m}_{e\beta} \propto \lambda^{n_\beta}, \quad \beta = e, \mu, \tau. \quad (72)$$



As follows from our analysis, we can have all  $e$ -row elements to be equal among themselves, simultaneously with equality of  $\mu\tau$ -block elements:

$$m \propto \begin{pmatrix} \lambda & \lambda & \lambda \\ \lambda & 1 & 1 \\ \lambda & 1 & 1 \end{pmatrix}, \quad (73)$$

where (see (26))

$$\lambda \approx \sqrt{2(s_{13}^2 + r^2 c_{12}^2 s_{12}^2)}.$$

For not too small  $s_{13}$  further structuring is possible, when  $m_{ee} \propto \lambda^2$ :

$$m \propto \begin{pmatrix} \lambda^2 & \lambda & \lambda \\ \lambda & 1 & 1 \\ \lambda & 1 & 1 \end{pmatrix}. \quad (74)$$

Such a situation is realized, *e.g.*, in Fig.2d (with certain shift of the  $e$ -row lines due to  $\delta$ ). In this case  $\lambda \approx s_{13}$ . The matrix (74) satisfies factorization condition. Other structuring of the  $e$ -row elements is also possible, like  $(\lambda^2, \lambda^2, \lambda)$  or  $(\lambda^2, \lambda, \lambda^2)$  with  $\lambda \approx 0.3$  (see Fig.3).

Mild hierarchy of elements in the  $\mu\tau$ -block is realized for non-maximal 2-3 mixing or/and non-trivial CP phases. According to Fig.3a,3b, we may have  $m_{\tau\tau} \approx m_{\mu\tau} > m_{\mu\mu} \approx m_{e\tau} > m_{e\mu} \approx m_{ee}$  which corresponds to parameterization:

$$m \propto \begin{pmatrix} \lambda^2 & \lambda^2 & \lambda \\ \lambda^2 & \lambda & 1 \\ \lambda & 1 & 1 \end{pmatrix}, \quad (75)$$

with  $\lambda \approx 0.3$ . Also  $m_{\tau\tau}$  can be the smallest element of the  $\mu\tau$ -block, instead of  $m_{\mu\mu}$ .

In the case of partial or complete degeneracy, new dominant structures appear and therefore new types of expansion is possible. According to Fig.6e and (63), the mass matrix can have the following form:

$$m \propto \begin{pmatrix} 1 & \lambda & \lambda \\ \lambda & 1 & 1 \\ \lambda & 1 & 1 \end{pmatrix}, \quad (76)$$

with

$$\lambda \approx \frac{s_{13}}{r\sqrt{2}}.$$

Two other possibilities are (see Figs.5f,6f):

$$m \propto \begin{pmatrix} 1 & \lambda & \lambda \\ \lambda & \lambda & 1 \\ \lambda & 1 & \lambda \end{pmatrix}, \quad m \propto \begin{pmatrix} 1 & \lambda & \lambda \\ \lambda & \lambda^2 & 1 \\ \lambda & 1 & \lambda^2 \end{pmatrix}, \quad (77)$$

with  $\lambda \approx s_{13}/\sqrt{2}$ , which should be taken of order 0.1 for the left matrix and 0.2 for the right matrix.

Notice that the value of  $\lambda$  which appears in the matrices (73)-(77) and, therefore, consistent with present data, can not be too small. We find

$$\lambda \gtrsim 0.1 - 0.2. \quad (78)$$

Values  $\sim 0.3 - 0.4$  are also allowed. The value of the parameter (78) can be equal to  $\sin \theta_c$ , where  $\theta_c$  is the Cabibbo angle, used as an expansion parameter for quark mass matrices. In the flavor basis the structure of the charge lepton mass matrix is characterized by the two ratios:  $m_\mu/m_\tau = 0.059$  and  $m_e/m_\mu = 0.0049$ . These ratios can also be reproduced as powers of  $\lambda$ :

$$m_e : m_\mu : m_\tau \approx \lambda^6 : \lambda^2 : 1,$$

with  $\lambda \approx 0.24$ .

In a large part of the parameter space, the elements of the mass matrix have the same order of magnitude, so that the ratio of matrix elements is close to 1. In this case we can introduce the ordering parameter  $\lambda_{ord} \sim \mathcal{O}(1)$ . Typical value of  $\lambda_{ord}$  can be determined, *e.g.*, by the possible spread of  $\mu\tau$ -block elements, due to deviation of the 2-3 mixing from maximal value:

$$\lambda_{ord} \approx \tan \theta_{23} \approx 0.7.$$

Another possible choice for  $\lambda_{ord}$ , in the partial degeneracy case, could be  $r$ . We find the following structures in Figs.2,3 (omitting the subscript ‘*ord*’):

$$m \propto \begin{pmatrix} \lambda^4 & \lambda^3 & \lambda^2 \\ \lambda^3 & \lambda^2 & \lambda \\ \lambda^2 & \lambda & 1 \end{pmatrix}, \quad m \propto \begin{pmatrix} \lambda^6 & \lambda^4 & \lambda^3 \\ \lambda^4 & \lambda^2 & \lambda \\ \lambda^3 & \lambda & 1 \end{pmatrix}. \quad (79)$$

These structures require rather large  $\theta_{13}$  to enhance the values of the  $e$ -row elements.

In the case of partial or complete degeneracy, situation appears where all elements are of the same order with small spread, see, *e.g.*, Fig.4f at  $\sigma \approx 0.7$ . In this connection one can consider the mass matrix as small deviation from the democratic one:

$$M \propto M^D + \Delta M ,$$

where  $|M_{\alpha\beta}^D| = 1$ ,  $\Delta M \sim \mathcal{O}(\lambda)$  and  $\lambda$  is a small parameter. Here  $\lambda$  can be taken of order  $s_{13}$  or  $\xi$  or  $1-r$  (deviation from degeneracy). An interesting possibility could be to take for  $\lambda$  the deviation of  $\rho$  or  $\sigma$  from the values  $0, \pi/2$ , which correspond to definite CP parities.

## 6.6 Symmetry basis

As we marked in the introduction, to get further theoretical inference, one needs to find the matrix in the symmetry basis and at the symmetry scale. In general, the symmetry basis differs from the flavor basis and the mass matrix of charged leptons  $M_l$  is non-diagonal there. The neutrino mass matrix in the symmetry basis,  $M_S$ , is related to that in flavor basis as  $M_S = U_l^T M U_l$ , where  $U_l$  is the mixing matrix which diagonalizes  $M_l$ . It may happen that due to strong hierarchy of the masses of the charged leptons, the charged lepton mixing is rather small and  $U_l \approx \mathbb{I}$ . In this case, the structures of the mass matrix  $M$ , discussed in this paper, are not modified significantly under transition to symmetry basis.

Let us mention another possibility. Being related to the ratio of masses of the muon and tau lepton, the 2-3 angle,  $\theta_{23}^l \sim \sqrt{m_\mu/m_\tau}$ , can be the only large angle in  $U_l$  (1-2 and 1-3 mixing angles are very small, if they are connected with the tiny electron mass). In this case, effect of charged lepton mixing on the neutrino mass matrix is reduced to change of the neutrino 2-3 angle in the flavor basis:

$$\theta_{23} = \theta_{23}^{sym} - \theta_{23}^l .$$

Taking into account this shift of the angle, one can use neutrino mass matrices obtained in this paper as mass matrices in the symmetry basis. This shift can justify large deviations of the neutrino 2-3 mixing from maximal value.

However, there are many models in which charged lepton mass matrix is strongly off-diagonal; see, *e.g.*, [9][10][33].

Structures of the mass matrix  $M$  will not be modified substantially due to running to high scales. It was found [34] that renormalization of  $M_{\alpha\beta}$  is smaller than  $10^{-4}$  for the Standard Model and about few percents for MSSM.

## 7 Discussion and conclusions

We have performed a systematic study of dependences of the neutrino mass matrix elements in the flavor basis on the CP violating phases. We have introduced the  $\rho - \sigma$  plots for the six independent masses, which show contours of constant mass in the plane of the Majorana phases  $\rho$  and  $\sigma$ . We used the  $\rho - \sigma$  plots to analyze the possible structures of the mass matrix. Our results can be summarized in the following way.

1) For strongly hierarchical mass spectrum ( $m_1 \approx 0$ ) and small  $s_{13}$ , the mass matrix has a structure with the dominant  $\mu\tau$ -block and small  $e$ -row elements. The ratio of masses of these two groups can be as small as 0.1.

The dominant structure becomes less profound for large  $\Delta m_{sol}^2$ , large  $s_{13}$  and significant deviation from maximal 2-3 mixing. For  $\Delta m_{sol}^2 > 2 \cdot 10^{-4} \text{ eV}^2$ , a separation of the elements in dominant block and sub-dominant  $e$ -row has no sense and one can consider certain non-hierarchical ordering of the elements. In particular, a configuration with nearly equal split among masses is possible.

2) The structure of the mass matrix changes significantly with increase of  $m_1$ . Already for partially degenerate spectrum, the gap between the  $\mu\tau$ -block elements and  $e$ -row elements disappears and all elements can be of the same order. Various equalities between the elements and orderings can be realized depending on the CP violating phases.

In the case of degenerate mass spectrum, the mass matrix can have a hierarchical structure with some elements (in particular, from the  $\mu\tau$ -block) being much smaller than other elements. We find that the hierarchical structures appear for specific ranges of phases.

In the case of complete degeneracy, the structure of the mass matrix is insensitive to the ordering of mass eigenvalues. Therefore, our conclusions are valid also for inverted ordering.

3) The Majorana phases  $\rho$  and  $\sigma$  and the Dirac phase  $\delta$  have different impact on the structure of the mass matrix. This impact depends on values of oscillation parameters.

(a) The Dirac phase  $\delta$  is associated with the small parameter  $s_{13}$ . The influence of this phase on the  $\mu\tau$ -block elements is relatively weak: it is suppressed by factor  $s_{13}$ . In contrast, the elements of  $e$ -row can be substantially influenced by  $\delta$ , especially in the case of hierarchical spectrum. In the first approximation  $\delta$  enters  $\tilde{m}_{e\mu}$  and  $\tilde{m}_{e\tau}$  in the combination  $(\delta - 2\sigma)$  and  $\tilde{m}_{ee}$  in the combination  $(2\delta - 2\sigma)$ . So, the effect of  $\delta$  is reduced to the appropriate shifts of phase  $\sigma$  for  $\tilde{m}_{ee}$ ,  $\tilde{m}_{e\mu}$  and  $\tilde{m}_{e\tau}$ . In this way one can change the

relative values of these elements with respect to the elements of  $\mu\tau$ -block. In the  $\rho-\sigma$  plot, for fixed pattern of the  $\mu\tau$ -block elements, the phase  $\delta$  produces a shift of the patterns for  $\tilde{m}_{e\mu}$  and  $\tilde{m}_{e\tau}$ , along the axis  $\sigma$ .

The phase  $\delta$  influences the relative values of  $\tilde{m}_{e\mu}$  and  $\tilde{m}_{e\tau}$ , but it has no strong impact on the dominant structure for any type of spectrum (hierarchical or degenerate). Improvements of the upper bound on  $s_{13}$  in future experiments will further suppress the influence of the Dirac phase on the structure of the mass matrix.

(b) The phase  $\rho$  is associated with the mass eigenvalue  $m_1$  and therefore, it has very small effect on the structure of the mass matrix in the case of hierarchical spectrum. The role of  $\rho$  increases with  $m_1$ . The influence of this phase depends on the solar mixing angle. It increases with  $\theta_{12}$ . Maximal impact is for maximal 1-2 mixing. Therefore future measurements of  $\theta_{12}$  in KAMLAND and solar neutrino experiments will allow one to further restrict the effect of  $\rho$  on the structure of the mass matrix.

For the best fit value of  $\theta_{12}$ , dependence of the  $\mu\tau$ -block elements on  $\rho$  is not very strong. However, existence of hierarchical structure (zeros) in this block is related to specific values of  $\rho$ . There is a strong dependence of the  $e$ -row elements on  $\rho$ . Typically  $\tilde{m}_{e\mu}$  and  $\tilde{m}_{e\tau}$  have minima at  $\rho \approx 0, \pi$  and they are maximal at  $\rho \approx \pi/2$ . The  $ee$ -element depends on  $\rho$  most strongly. There is a chance to measure/restrict  $\rho$  in the  $\beta\beta_{0\nu}$ -decay searches, provided that the absolute mass scale will be determined (further restricted) in the direct kinematic measurements.

(c) The phase  $\sigma$  is associated with the heaviest mass eigenstate and, consequently, the  $\sigma$ -dependence is strong for all the elements but  $\tilde{m}_{ee}$ . Variations of the  $ee$ -element with  $\sigma$  are suppressed by a factor  $s_{13}^2$ .

The phase  $\sigma$  enters the  $e$ -row elements,  $\tilde{m}_{e\mu}$  and  $\tilde{m}_{e\tau}$  with a factor  $s_{13}$ . In spite of this, in the case of hierarchical spectrum variations of  $\tilde{m}_{e\mu}$  and  $\tilde{m}_{e\tau}$  with  $\sigma$  can be strong. With increase of  $r$ , the relative amplitude of variations of these elements with  $\sigma$  decreases. In contrast, the dependence of  $\mu\tau$ -block elements on  $\sigma$  becomes stronger with increase of  $r$ . It can be enhanced, in addition, if the 2-3 mixing is non-maximal. In the case of degenerate spectrum, variations of the  $\mu\tau$ -block elements with  $\sigma$  can be maximal, so that, at certain values of phases, a given element can be zero or the largest one.

4) There are correlations among the dependences of the matrix elements on phases. In general, patterns of  $\tilde{m}_{\mu\mu}$  and  $\tilde{m}_{\tau\tau}$  are complementary to the pattern of  $\tilde{m}_{\mu\tau}$ . The patterns for  $\tilde{m}_{e\mu}$  and  $\tilde{m}_{e\tau}$  are shifted by  $\Delta\sigma = \pi/2$ , etc.

Dominant structures of the mass matrix can be identified considering the limit  $s_{13} \rightarrow 0$ .

The terms of order  $s_{13}$  give small corrections to the dominant elements. In contrast, the  $s_{13}$ -order terms can be important or even give main contribution to the sub-leading elements of the mass matrix. Obviously, the phase  $\delta$  does not determine the dominant structure.

In the case of hierarchical mass spectrum the dominant structure is formed by the  $\mu\tau$ -block (see Eq. (57)). Properties of this block depend on the 2-3 mixing and on the phase  $\sigma$ . For partially degenerate or degenerate spectrum the dominant structures can be obtained by Eq.(48). For a given value of the mass ratio  $r$ , the structure is determined by  $x$  and the unique phase  $\sigma_X$ , which can be considered as independent parameters. Moreover, the  $e$ -row elements do not depend on  $\sigma_X$ .

Using Eq.(48) it is easy to identify all possible structures of the mass matrices in the first approximation (possible hierarchical mass matrices, matrices with approximately equal elements, etc.).

5) We have found that the mass matrix has a hierarchical structure:

(a) In the case of hierarchical mass spectrum: the  $e$ -row elements can be about 10 times smaller than the  $\mu\tau$ -block elements.

(b) In the case of degenerate mass spectrum: the hierarchy determined by a factor  $\sim 10$  or more appears in the regions near the corners of the  $\rho - \sigma$  plots:

$$\rho \approx 0 - \pi/8, \quad \sigma \approx 0 - \pi/32,$$

for the first corner, and similar interval for the three other corners. In these cases the matrix equals approximately to the unit matrix with small off-diagonal terms. Another possibility is

$$\rho \approx 0 - \pi/6, \quad \sigma \approx (0.45 - 0.55) \pi$$

and similar reflected region  $\rho \rightarrow \pi - \rho$ . In this case the mass matrix has a dominant structure with  $\tilde{m}_{ee} \approx \tilde{m}_{\mu\tau}$ , while all other elements are small.

(c) For non-maximal 2-3 mixing: the element  $\tilde{m}_{\mu\mu}$  or  $\tilde{m}_{\tau\tau}$  can be small for  $\sigma \approx \pi/2$  and for a value of  $\rho$  which depends on the deviation  $\xi$  of 2-3 mixing from maximal value. With increase of  $\xi$ , the region of small mass approaches the center of  $\rho - \sigma$  plots ( $\rho \sim \pi/2$ ).

Typical separations among the elements in the hierarchical structures of the neutrino mass matrix are characterized by a factor 0.2 - 0.3. We have found that it is possible to parameterize the matrix by powers of a single parameter  $\lambda$  (whose origin can be in the breaking of some flavor symmetry at high energy). The value  $\lambda \approx 0.2 - 0.3$  is consistent with the Cabibbo angle and also it can be related to the ratios of charge lepton masses.

If 2-3 mixing is not maximal, one can introduce an ordering parameter  $\lambda_{ord} \sim \tan \theta_{23} \sim 0.6 - 0.7$ . We find that the whole matrix can be parametrized in terms of powers of this ordering parameter.

The democratic mass matrix and matrices with flavor disordering are possible.

6) The following results from forthcoming experiments will have crucial impact on the structure of the neutrino mass matrix:

- improvement of bound on (or determination of) the deviation from maximal 2-3 mixing;
- precise determination of the solar oscillation parameters,  $\Delta m_{sol}^2$  and  $\theta_{12}$ ;
- improvement of bound on (or determination of)  $s_{13}$ ;
- improvement of bound on (or determination of)  $m_{ee}$ ;
- direct kinematic measurements of the neutrino mass.

The double beta decay searches play a special role in the determination of mass matrix structure. If these searches give a positive result and also future direct measurements improve the bound on (or measure)  $m_1$ , we will be able to select a narrow strip in the  $\rho - \sigma$  diagram. This will also determine other  $e$ -row elements. However, the value of the  $\mu\tau$ -block elements will be largely undetermined, due to their strong dependence on the unknown phase  $\sigma$ .

## Appendix A: Analytic expressions for matrix elements

The neutrino mass matrix elements in flavor basis,  $M_{\alpha\beta}$  ( $\alpha, \beta = e, \mu, \tau$ ), are functions of the mass eigenvalues  $m_i$ , of the mixing angles  $\theta_{ij}$  and of the CP violating phases  $\delta, \rho, \sigma$  (see (4)).

Denoting  $c_{ij} \equiv \cos \theta_{ij}$  and  $s_{ij} \equiv \sin \theta_{ij}$ , we get the following expressions for the matrix elements, as sums of three terms corresponding to the three mass eigenstates:

$$M_{ee} = c_{13}^2 c_{12}^2 m_1 e^{-2i\rho} + c_{13}^2 s_{12}^2 m_2 + s_{13}^2 m_3 e^{2i(\delta-\sigma)} ; \quad (\text{A.1})$$

$$M_{e\mu} = c_{13} c_{12} (-c_{23} s_{12} - s_{23} c_{12} s_{13} e^{-i\delta}) m_1 e^{-2i\rho} + c_{13} s_{12} (c_{23} c_{12} - s_{23} s_{12} s_{13} e^{-i\delta}) m_2 + c_{13} s_{23} s_{13} m_3 e^{i(\delta-2\sigma)} ; \quad (\text{A.2})$$

$$\begin{aligned}
M_{e\tau} = & c_{13} c_{12} (s_{23} s_{12} - c_{23} c_{12} s_{13} e^{-i\delta}) m_1 e^{-2i\rho} + \\
& c_{13} s_{12} (-s_{23} c_{12} - c_{23} s_{12} s_{13} e^{-i\delta}) m_2 + \\
& c_{13} c_{23} s_{13} m_3 e^{i(\delta-2\sigma)} ;
\end{aligned} \tag{A.3}$$

$$\begin{aligned}
M_{\mu\mu} = & (-c_{23} s_{12} - s_{23} c_{12} s_{13} e^{-i\delta})^2 m_1 e^{-2i\rho} + \\
& (c_{23} c_{12} - s_{23} s_{12} s_{13} e^{-i\delta})^2 m_2 + \\
& c_{13}^2 s_{23}^2 m_3 e^{-2i\sigma} ;
\end{aligned} \tag{A.4}$$

$$\begin{aligned}
M_{\mu\tau} = & (s_{23} s_{12} - c_{23} c_{12} s_{13} e^{-i\delta}) (-c_{23} s_{12} - s_{23} c_{12} s_{13} e^{-i\delta}) m_1 e^{-2i\rho} + \\
& (-s_{23} c_{12} - c_{23} s_{12} s_{13} e^{-i\delta}) (c_{23} c_{12} - s_{23} s_{12} s_{13} e^{-i\delta}) m_2 + \\
& c_{13}^2 c_{23} s_{23} m_3 e^{-2i\sigma} ;
\end{aligned} \tag{A.5}$$

$$\begin{aligned}
M_{\tau\tau} = & (s_{23} s_{12} - c_{23} c_{12} s_{13} e^{-i\delta})^2 m_1 e^{-2i\rho} + \\
& (-s_{23} c_{12} - c_{23} s_{12} s_{13} e^{-i\delta})^2 m_2 + \\
& c_{13}^2 c_{23}^2 m_3 e^{-2i\sigma} .
\end{aligned} \tag{A.6}$$

It is convenient to use also a representation of the matrix elements as series in powers of  $s_{13}$ . Using the equations (A.1)-(A.6) and the definitions (28), we get:

$$\begin{aligned}
\tilde{M}_{ee} &= rZ + s_{13}^2 Z' , \\
\tilde{M}_{e\mu} &= c_{13}(c_{23}rY + s_{13}s_{23}e^{-i\delta}Z') , \\
\tilde{M}_{e\tau} &= c_{13}(-s_{23}rY + s_{13}c_{23}e^{-i\delta}Z') , \\
\tilde{M}_{\mu\mu} &= c_{23}^2 Xr + s_{23}^2 e^{-2i\sigma} - \sin 2\theta_{23}s_{13}r e^{-i\delta}Y - s_{23}^2 s_{13}^2 e^{-2i\delta}Z' , \\
\tilde{M}_{\tau\tau} &= s_{23}^2 Xr + c_{23}^2 e^{-2i\sigma} + \sin 2\theta_{23}s_{13}r e^{-i\delta}Y - c_{23}^2 s_{13}^2 e^{-2i\delta}Z' , \\
\tilde{M}_{\mu\tau} &= s_{23}c_{23}(-rX + e^{-2i\sigma}) - \cos 2\theta_{23}s_{13}r e^{-i\delta}Y - s_{23}c_{23}s_{13}^2 e^{-2i\delta}Z' ,
\end{aligned} \tag{A.7}$$

where

$$Z' \equiv e^{2i(\delta-\sigma)} - rZ . \tag{A.8}$$

We will use also another form for the matrix elements, which is obtained neglecting terms of the order  $s_{13}^2$ . For the  $\mu\tau$ -block, we get:

$$\begin{aligned}
\tilde{m}_{\mu\mu} &\approx |s_{23}^2 e^{-2i\sigma} + r c_{23}^2 (c_{12}^2 - \epsilon_{\mu\mu}) + k r c_{23}^2 (s_{12}^2 + \epsilon_{\mu\mu}) e^{-2i\rho}| , \\
\tilde{m}_{\tau\tau} &\approx |c_{23}^2 e^{-2i\sigma} + r s_{23}^2 (c_{12}^2 + \epsilon_{\tau\tau}) + k r s_{23}^2 (s_{12}^2 - \epsilon_{\tau\tau}) e^{-2i\rho}| , \\
\tilde{m}_{\mu\tau} &\approx s_{23} c_{23} |-e^{-2i\sigma} + r (c_{12}^2 + \epsilon_{\mu\tau}) + k r (s_{12}^2 - \epsilon_{\mu\tau}) e^{-2i\rho}| ,
\end{aligned} \tag{A.9}$$



where

$$\epsilon_{\alpha\beta}(\delta) = \sin 2\theta_{12}s_{13}e^{-i\delta} \times \begin{cases} \tan \theta_{23}, & \epsilon_{\mu\mu} \\ \cot \theta_{23}, & \epsilon_{\tau\tau} \\ \cot 2\theta_{23}, & \epsilon_{\mu\tau} \end{cases} . \quad (\text{A.10})$$

Notice that the three different terms in the Eqs.(A.9) are contributions of the three masses  $m_3$ ,  $m_2$  and  $m_1$ . For the elements of the  $e$ -row we get, up to an overall factor  $c_{13}$ :

$$\begin{aligned} \tilde{m}_{e\mu} &\approx \left| rc_{12}s_{12}c_{23} \left[ 1 - \epsilon_{e\mu} - ke^{-2i\rho}(1 + \epsilon'_{e\mu}) \right] + s_{13}s_{23}e^{i(\delta-2\sigma)} \right|, \\ \tilde{m}_{e\tau} &\approx \left| rc_{12}s_{12}s_{23} \left[ 1 + \epsilon_{e\tau} - ke^{-2i\rho}(1 - \epsilon'_{e\tau}) \right] - s_{13}c_{23}e^{i(\delta-2\sigma)} \right|, \end{aligned} \quad (\text{A.11})$$

where

$$\begin{aligned} (\epsilon_{e\mu}, \epsilon'_{e\mu}) &= s_{13}e^{-i\delta} \tan \theta_{23} \times (\tan \theta_{12}, \cot \theta_{12}), \\ (\epsilon_{e\tau}, \epsilon'_{e\tau}) &= s_{13}e^{-i\delta} \cot \theta_{23} \times (\tan \theta_{12}, \cot \theta_{12}). \end{aligned} \quad (\text{A.12})$$

The  $ee$ -element can be written as

$$\tilde{m}_{ee} = \left| c_{13}^2(c_{12}^2ke^{-2i\rho} + s_{12}^2)r + s_{13}^2e^{2i(\delta-\sigma)} \right|. \quad (\text{A.13})$$

It does not depend on the angle  $\theta_{23}$ .

## Appendix B: Dependence of mass matrix on $m_1$

We present here some analytic study and comment on the particular structures shown in Fig.6.

Let us consider first the case  $\rho = 0$ , which corresponds to same CP parities of  $\nu_1$  and  $\nu_2$  (see Fig.6 panels a,e,f). From (39,42,45), we get:

$$Y_1 = 0, \quad X_1 = Z_1 = 1.$$

Consequently (see (38,43,44)):

$$\tilde{m}_{\mu\mu} \approx \left| s_{23}^2e^{-2i\sigma} + rc_{23}^2 \right|, \quad \tilde{m}_{\tau\tau} \approx \left| c_{23}^2e^{-2i\sigma} + rs_{23}^2 \right|, \quad \tilde{m}_{\mu\tau} \approx s_{23}c_{23} \left| e^{-2i\sigma} - r \right|, \quad (\text{B.1})$$

$$\tilde{m}_{e\mu} = \tan \theta_{23}\tilde{m}_{e\tau} \approx s_{13}s_{23} \left| 1 - re^{2i(\sigma-\delta)} \right|, \quad \tilde{m}_{ee} \approx r. \quad (\text{B.2})$$

The elements  $m_{e\mu}$  and  $m_{e\tau}$  are parametrically suppressed with respect to the others by a factor  $s_{13}$ . The  $ee$ -element does not depend on phases in this approximation.

Let us consider also specific values of the phase  $\sigma$ .

1)  $\sigma = 0$ , all states have the same CP-parities (Fig.6a). With increase of  $m_1$  ( $r \rightarrow 1$ ), the diagonal elements converge to 1, whereas the off-diagonal elements decrease, if  $\delta = 0$ . The matrix approaches the unit matrix.

2)  $\sigma = \pi/4$  (Fig.6e). In this case (if  $\delta = 0$ ):

$$\begin{aligned}\tilde{m}_{\mu\mu} &= \sqrt{s_{23}^4 + r^2 c_{23}^4}, & \tilde{m}_{\tau\tau} &= \sqrt{c_{23}^4 + r^2 s_{23}^4}, & \tilde{m}_{\mu\tau} &= s_{23} c_{23} \sqrt{1 + r^2}, \\ \tilde{m}_{e\mu} &= \tan \theta_{23} \tilde{m}_{e\tau} = s_{13} s_{23} \sqrt{1 + r^2}.\end{aligned}$$

For maximal 2-3 mixing, we get

$$\tilde{m}_{\mu\mu} = \tilde{m}_{\tau\tau} = \tilde{m}_{\mu\tau} = \frac{1}{2} \sqrt{1 + r^2}.$$

If  $r^2 \approx 1/3$ , also  $m_{ee}$  is equal to the  $\mu\tau$ -block elements.

3)  $\sigma = \pi/2$ , that is,  $\nu_3$  and  $\nu_2$  have opposite CP-parities (Fig.6f). We find, for maximal 2-3 mixing and  $\delta = 0$ :

$$\tilde{m}_{\mu\mu} = \tilde{m}_{\tau\tau} = \frac{1}{2}(1 - r), \quad \tilde{m}_{\mu\tau} = \frac{1}{2}(1 + r), \quad \tilde{m}_{e\mu} = \tilde{m}_{e\tau} = s_{13} \sqrt{\frac{1 + r^2}{2}}.$$

So, for  $r \rightarrow 1$ ,  $\tilde{m}_{\mu\mu} = \tilde{m}_{\tau\tau} \rightarrow 0$  and  $\tilde{m}_{\mu\tau} \rightarrow 1$ .

Let us consider the case  $\rho = \pi/2$ , which corresponds to opposite CP parities of  $\nu_1$  and  $\nu_2$  (see Fig.6 panels b,d). From Eqs.(39,42,45) we get:

$$Y_1 = \sin 2\theta_{12}, \quad X_1 = -Z_1 = \cos 2\theta_{12}. \quad (\text{B.3})$$

Then, the elements of  $\mu\tau$ -block are given in Eq.(40); for maximal 2-3 mixing and  $\delta = 0$  (the case shown in the Fig.6), the expressions (40) reduce to:

$$\begin{aligned}\tilde{m}_{\mu\mu} &\approx \frac{1}{2} |e^{-2i\sigma} + r(\cos 2\theta_{12} - 2\epsilon_0)|, \\ \tilde{m}_{\tau\tau} &\approx \frac{1}{2} |e^{-2i\sigma} + r(\cos 2\theta_{12} + 2\epsilon_0)|, \\ \tilde{m}_{\mu\tau} &\approx \frac{1}{2} |e^{-2i\sigma} - r \cos 2\theta_{12}|,\end{aligned}$$

where  $\epsilon_0 \equiv \sin 2\theta_{12} s_{13}$ . The elements  $\tilde{m}_{\mu\mu}$  and  $\tilde{m}_{\tau\tau}$  differ due to corrections  $\epsilon_0$ :

$$\frac{\tilde{m}_{\mu\mu} - \tilde{m}_{\tau\tau}}{m_{\mu\mu}} \sim \frac{4s_{13}r \sin 2\theta_{12}}{|r \cos 2\theta_{12} + e^{-2i\sigma}|}. \quad (\text{B.4})$$

For maximal 2-3 mixing, the  $e$ -row elements are given by (see (A.11)):

$$\tilde{m}_{e\mu} \approx \frac{1}{\sqrt{2}} |r \sin 2\theta_{12} + f|, \quad \tilde{m}_{e\tau} \approx \frac{1}{\sqrt{2}} |r \sin 2\theta_{12} - f|,$$

where

$$f \equiv s_{13} e^{-i\delta} (r \cos 2\theta_{12} + e^{2i(\delta-\sigma)}) .$$

So, the split of these elements is described by

$$\frac{\tilde{m}_{e\mu} - \tilde{m}_{e\tau}}{\tilde{m}_{e\mu}} \sim \frac{2f}{r \sin 2\theta_{12}} . \quad (\text{B.5})$$

Finally, the  $ee$ -element equals

$$\tilde{m}_{ee} \approx \cos 2\theta_{12} r .$$

The elements  $m_{ee}$  and  $m_{\mu\tau}$  have no order  $s_{13}$  corrections.

Let us consider particular values of  $\sigma$  (and  $\delta = 0$ ):

1)  $\sigma = 0$  (Fig.6b). There is a substantial split between  $\tilde{m}_{\mu\mu}$  and  $\tilde{m}_{\tau\tau}$ :  $4s_{13} \tan \theta_{12}$ , in the limit  $r = 1$ . The split between  $\tilde{m}_{e\mu}$  and  $\tilde{m}_{e\tau}$  is also relatively large:  $2s_{13} \cot \theta_{12}$ , in the limit  $r = 1$ .

2)  $\sigma = \pi/2$  (Fig.6d). The two terms in  $\tilde{m}_{\mu\tau}$  add, whereas they cancel in  $\tilde{m}_{\mu\mu}$  and  $\tilde{m}_{\tau\tau}$ . Now  $\tilde{m}_{e\tau} > \tilde{m}_{e\mu}$ , because  $f < 0$ ; for best fit value of 1-2 mixing, the split is smaller than in the case of  $\sigma = 0$ :  $2s_{13} \tan \theta_{12}$ , in the limit  $r = 1$ .

For  $\rho = \pi/4$  and  $s_{13} = \xi = 0$  (Fig.6c), the elements of  $e$ -row do not depend on  $\sigma$ :

$$\tilde{m}_{ee} = r \sqrt{s_{12}^4 + c_{12}^4} , \quad \tilde{m}_{e\mu} = \tilde{m}_{e\tau} = r s_{12} c_{12} .$$

In contrast, the  $\mu\tau$ -block elements are  $\sigma$ -dependent. For  $\sigma = \pi/4$  (Fig.6c):

$$\tilde{m}_{\mu\mu} = \tilde{m}_{\tau\tau} = \frac{1}{2} \sqrt{1 + r^2 + 2s_{12}^2 r (1 - r c_{12}^2)} , \quad \tilde{m}_{\mu\tau} = \frac{1}{2} \sqrt{1 + r^2 - 2s_{12}^2 r (1 + r c_{12}^2)} .$$

In the limit of strong degeneracy,  $r \rightarrow 1$ ,

$$\tilde{m}_{\mu\mu} = \tilde{m}_{\tau\tau} = \sqrt{\frac{1 + s_{12}^4}{2}} , \quad \tilde{m}_{\mu\tau} = \frac{c_{12}^2}{\sqrt{2}} .$$

This gives  $m_{e\mu} < m_{\mu\tau} < m_{\mu\mu} < m_{ee}$  for LMA best fit value of  $\theta_{12}$ . Other orderings are possible for  $\sigma \neq \pi/4$ .

## References

- [1] Y. Fukuda *et al.* [SuperKamiokande Collaboration], Phys. Lett. B **467** (1999) 185 [hep-ex/9908049]; S. Fukuda *et al.* [Super-Kamiokande Collaboration], Phys. Rev. Lett. **85** (2000) 3999 [hep-ex/0009001]; T. Toshito [SuperKamiokande Collaboration], hep-ex/0105023.

- [2] S. Fukuda *et al.* [SuperKamiokande Collaboration], Phys. Rev. Lett. **86** (2001) 5651 [hep-ex/0103032]; Phys. Rev. Lett. **86** (2001) 5656 [hep-ex/0103033].
- [3] Q. R. Ahmad *et al.* [SNO Collaboration], Phys. Rev. Lett. **87** (2001) 071301 [nucl-ex/0106015].
- [4] C. D. Froggatt and H. B. Nielsen, Nucl. Phys. B **147** (1979) 277.
- [5] E. Papageorgiu, Z. Phys. C **64** (1994) 509 [hep-ph/9405256]; P. Binetruy, S. Lavignac and P. Ramond, Nucl. Phys. B **477** (1996) 353 [hep-ph/9601243]; J. K. Elwood, N. Irges and P. Ramond, Phys. Rev. Lett. **81** (1998) 5064 [hep-ph/9807228]; G. Altarelli and F. Feruglio, Phys. Lett. B **451** (1999) 388 [hep-ph/9812475]; S. Lola and G. G. Ross, Nucl. Phys. B **553** (1999) 81 [hep-ph/9902283]; S. F. King, Nucl. Phys. B **576** (2000) 85 [hep-ph/9912492]; K. Choi, E. J. Chun, K. Hwang and W. Y. Song, Phys. Rev. D **64** (2001) 113013 [hep-ph/0107083].
- [6] G. Altarelli and F. Feruglio, Phys. Rept. **320** (1999) 295.
- [7] D. B. Kaplan and M. Schmaltz, Phys. Rev. D **49** (1994) 3741 [hep-ph/9311281]; M. Fukugita, M. Tanimoto and T. Yanagida, Phys. Rev. D **57** (1998) 4429 [hep-ph/9709388]; Z. Berezhiani and A. Rossi, JHEP **9903** (1999) 002 [hep-ph/9811447] and Nucl. Phys. Proc. Suppl. **101** (2001) 410 [hep-ph/0107054]; P. H. Frampton and A. Rasin, Phys. Lett. B **478** (2000) 424 [hep-ph/9910522].
- [8] H. Fritzsch and Z. z. Xing, Prog. Part. Nucl. Phys. **45** (2000) 1 [hep-ph/9912358].
- [9] S. M. Barr and I. Dorsner, Nucl. Phys. B **585** (2000) 79 [hep-ph/0003058].
- [10] R. Barbieri, L. J. Hall, D. R. Smith, A. Strumia and N. Weiner, JHEP **9812** (1998) 017 [hep-ph/9807235]; R. Barbieri, L. J. Hall and A. Strumia, Phys. Lett. B **445** (1999) 407 [hep-ph/9808333].
- [11] F. Vissani, JHEP **9811** (1998) 025 [hep-ph/9810435]; Phys. Lett. B **508** (2001) 79 [hep-ph/0102236]; hep-ph/0111373.
- [12] E. K. Akhmedov, Phys. Lett. B **467** (1999) 95 [hep-ph/9909217]; A. Abada and M. Losada, Nucl. Phys. B **585** (2000) 45 [hep-ph/9908352]; T. Hambye, hep-ph/0201307; H. V. Klapdor-Kleingrothaus and U. Sarkar, hep-ph/0202006.

- [13] M. Apollonio *et al.* [CHOOZ Collaboration], Phys. Lett. B **420** (1998) 397 [hep-ex/9711002]; Phys. Lett. B **466** (1999) 415 [hep-ex/9907037]. See also: F. Boehm *et al.*, Phys. Rev. D **64** (2001) 112001 [hep-ex/0107009].
- [14] J. Sato and T. Yanagida, Phys. Lett. B **493** (2000) 356 [hep-ph/0009205].
- [15] F. Feruglio, A. Strumia and F. Vissani, hep-ph/0201291.
- [16] P. H. Frampton, S. L. Glashow and D. Marfatia, hep-ph/0201008; Z. z. Xing, hep-ph/0201151.
- [17] H. Fritzsch and Z. Z. Xing, Phys. Lett. B **372** (1996) 265 [hep-ph/9509389]; G. C. Branco, M. N. Rebelo and J. I. Silva-Marcos, Phys. Rev. D **62** (2000) 073004 [hep-ph/9906368]; E. K. Akhmedov, G. C. Branco, F. R. Joaquim and J. I. Silva-Marcos, Phys. Lett. B **498** (2001) 237 [hep-ph/0008010]; K. Fukuura, T. Miura, E. Takasugi and M. Yoshimura, Phys. Rev. D **61** (2000) 073002 [hep-ph/9909415].
- [18] L. J. Hall, H. Murayama and N. Weiner, Phys. Rev. Lett. **84** (2000) 2572 [hep-ph/9911341]; N. Haba and H. Murayama, Phys. Rev. D **63** (2001) 053010 [hep-ph/0009174].
- [19] S. Lavignac, I. Masina and C. A. Savoy, hep-ph/0202086.
- [20] K. Zuber, hep-ph/0008080.
- [21] A. Y. Smirnov, D. N. Spergel and J. N. Bahcall, Phys. Rev. D **49** (1994) 1389 [hep-ph/9305204]; B. Jegerlehner, F. Neubig and G. Raffelt, Phys. Rev. D **54** (1996) 1194 [astro-ph/9601111]; H. Minakata and H. Nunokawa, Phys. Lett. B **504** (2001) 301 [hep-ph/0010240]; C. Lunardini and A. Y. Smirnov, Nucl. Phys. B **616** (2001) 307 [hep-ph/0106149].
- [22] V. Barger, D. Marfatia and B. P. Wood, hep-ph/0202158.
- [23] G. L. Fogli, E. Lisi, D. Montanino and A. Palazzo, Phys. Rev. D **64** (2001) 093007 [hep-ph/0106247]; A. Bandyopadhyay, S. Choubey, S. Goswami and K. Kar, Phys. Lett. B **519** (2001) 83 [hep-ph/0106264]; J. N. Bahcall, M. C. Gonzalez-Garcia and C. Pena-Garay, JHEP **0108** (2001) 014 [hep-ph/0106258]; P. I. Krastev and A. Y. Smirnov, hep-ph/0108177; P. Aliani, V. Antonelli, M. Picariello and E. Torrente-Lujan, hep-ph/0111418.

- [24] A. Piepke [KamLAND Collaboration], Nucl. Phys. Proc. Suppl. **91** (2001) 99; V. D. Barger, D. Marfatia and B. P. Wood, Phys. Lett. B **498** (2001) 53 [hep-ph/0011251]; A. de Gouvea and C. Pena-Garay, Phys. Rev. D **64** (2001) 113011 [hep-ph/0107186].
- [25] J. Bonn *et al.*, Nucl. Phys. Proc. Suppl. **91** (2001) 273.
- [26] H. V. Klapdor-Kleingrothaus *et al.*, hep-ph/0103062; H. V. Klapdor-Kleingrothaus [Heidelberg-Moscow Collaboration], hep-ph/0103074.
- [27] C. E. Aalseth *et al.*, hep-ex/0202026.
- [28] H. V. Klapdor-Kleingrothaus, A. Dietz, H. L. Harney and I. V. Krivosheina, Mod. Phys. Lett. A **16** (2002) 2409 [hep-ph/0201231].
- [29] C. E. Aalseth *et al.*, hep-ex/0202018.
- [30] H. V. Klapdor-Kleingrothaus, H. Pas and A. Y. Smirnov, Phys. Rev. D **63** (2001) 073005 [hep-ph/0003219].
- [31] H. Minakata and O. Yasuda, Phys. Rev. D **56** (1997) 1692 [hep-ph/9609276].
- [32] A. Osipowicz *et al.* [KATRIN Collaboration], hep-ex/0109033.
- [33] K. S. Babu and S. M. Barr, Phys. Lett. B **525** (2002) 289 [hep-ph/0111215].
- [34] K. S. Babu, C. N. Leung and J. Pantaleone, Phys. Lett. B **319** (1993) 191 [hep-ph/9309223]; J. R. Ellis and S. Lola, Phys. Lett. B **458** (1999) 310 [hep-ph/9904279]; J. A. Casas, J. R. Espinosa, A. Ibarra and I. Navarro, Nucl. Phys. B **573** (2000) 652 [hep-ph/9910420]; S. Antusch, M. Drees, J. Kersten, M. Lindner and M. Ratz, Phys. Lett. B **519** (2001) 238 [hep-ph/0108005]; P. H. Chankowski and S. Pokorski, hep-ph/0110249.

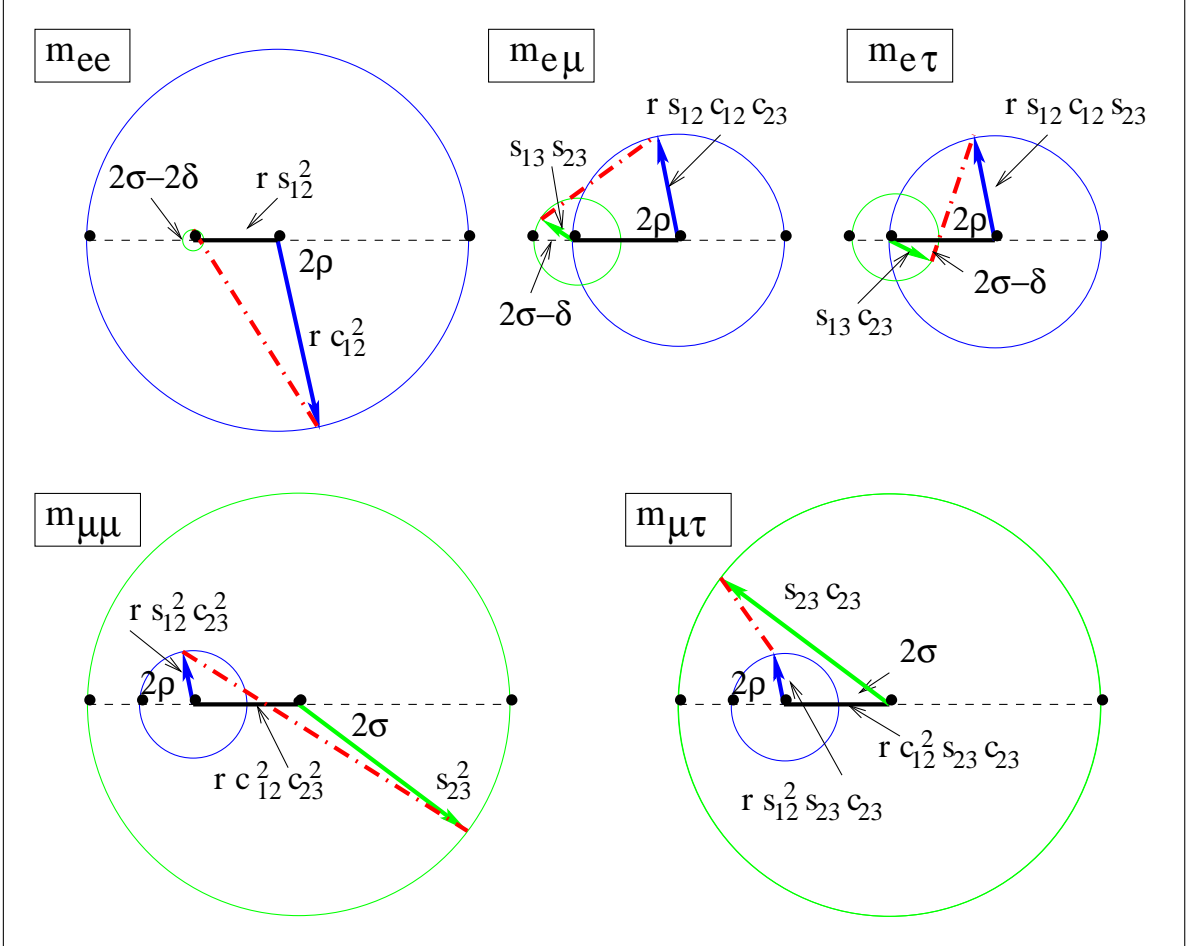


Figure 1: Phase diagrams. Shown is a graphic representation of the mass matrix elements  $m_{\alpha\beta}$  in the complex plane. Thick lines represent the contributions of the three leading terms in expressions (A.9,A.11,A.13). The diagram for  $m_{\tau\tau}$  is obtained from the  $m_{\mu\mu}$  diagram with the substitution  $s_{23} \leftrightarrow c_{23}$ . The length of the dash-dotted line gives the value of the matrix element. The diagrams correspond to the spectrum with partial degeneracy ( $k \approx 1$ ,  $r \lesssim 1$ ).

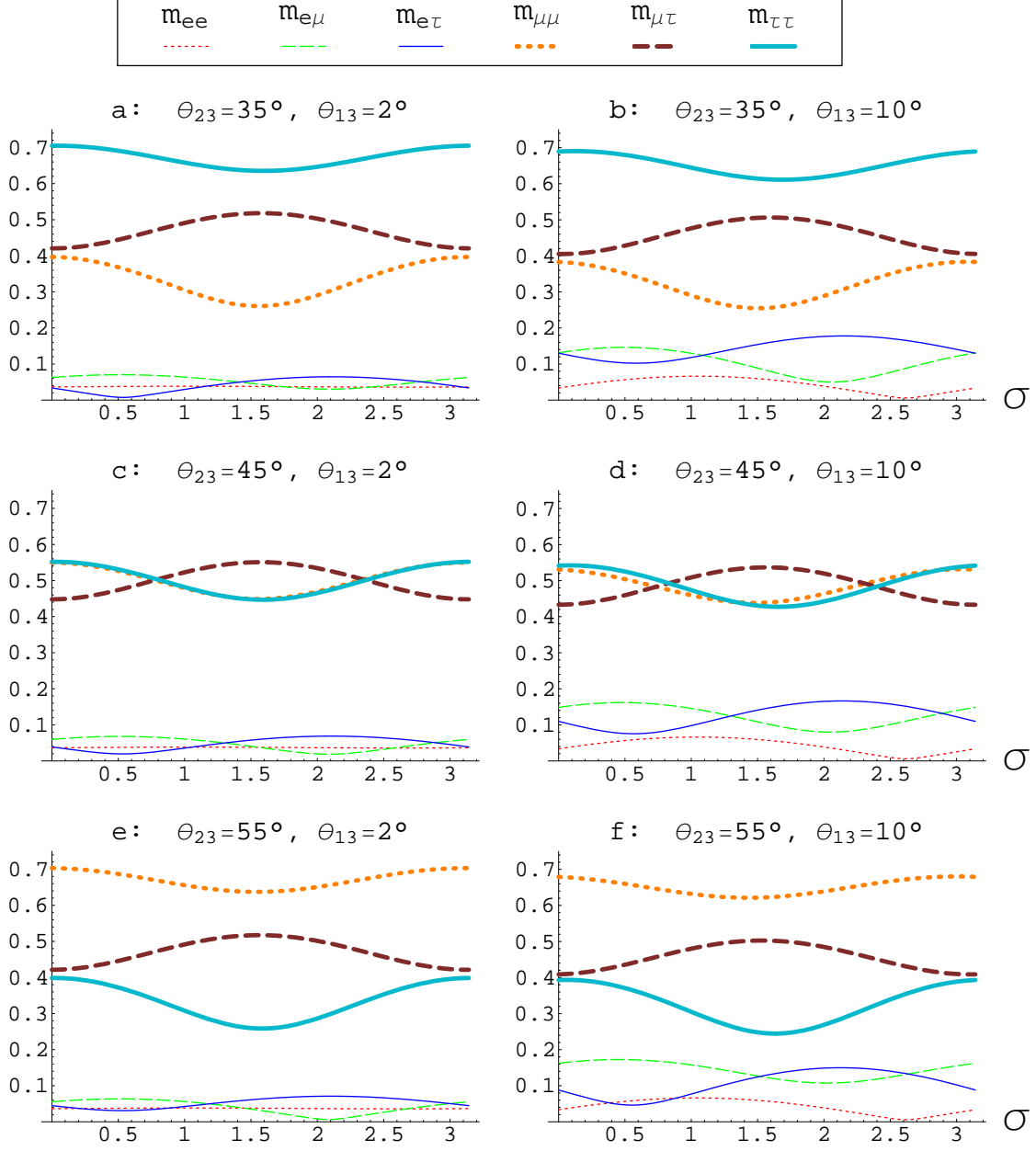


Figure 2: Dependence of the absolute value of neutrino mass matrix elements (in units  $\sqrt{\Delta m_{atm}^2} = 0.05$  eV) on  $\sigma$ , for different values of  $\theta_{23}$  and  $\theta_{13}$ . We take  $\tan^2 \theta_{12} = 0.36$ ,  $\delta = \pi/3$ ,  $m_2 = 0.14 m_3$ ,  $m_1 = 0$ .



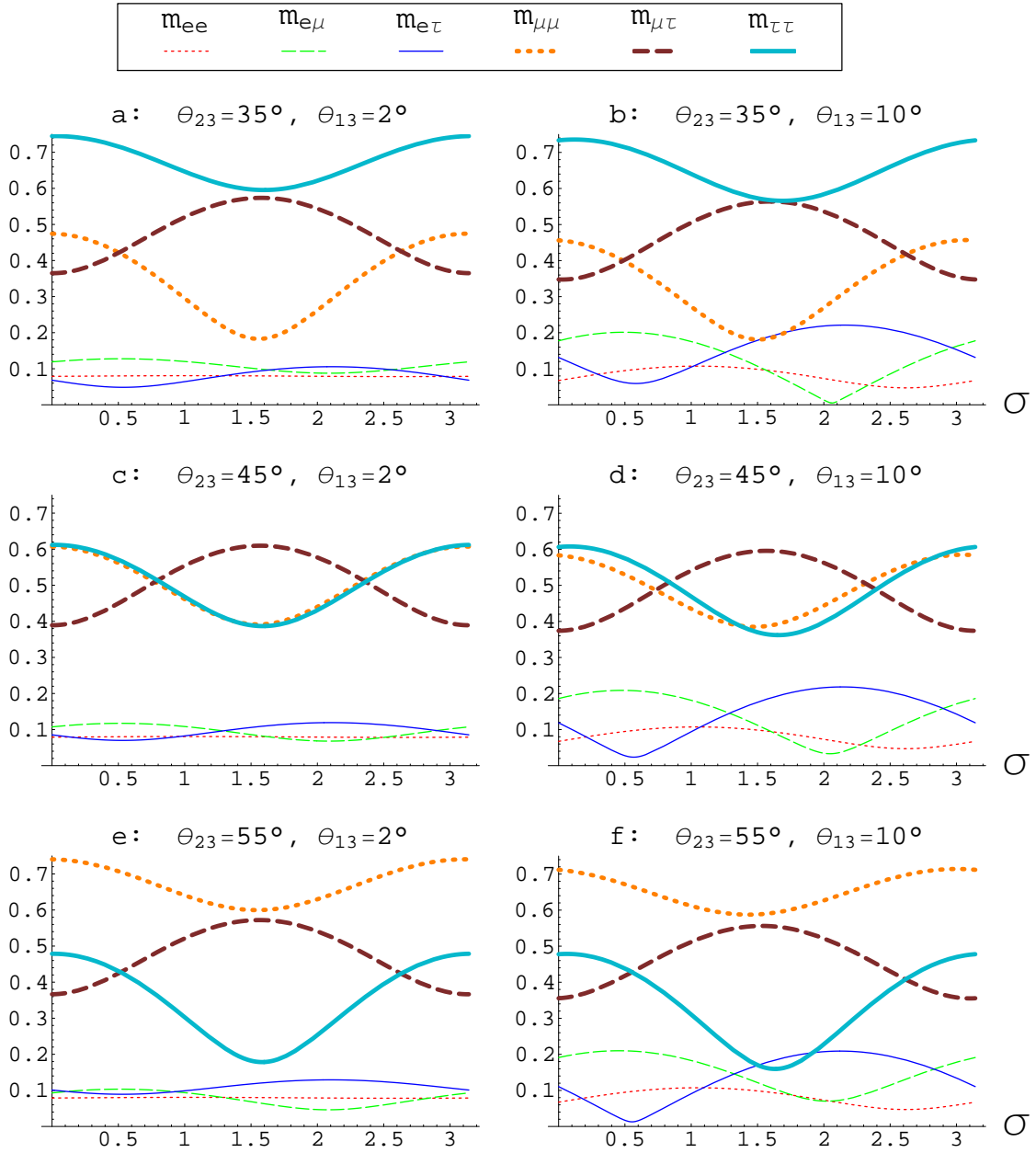


Figure 3: The same as in Fig.2, but for  $m_2 = 0.3 m_3$ .

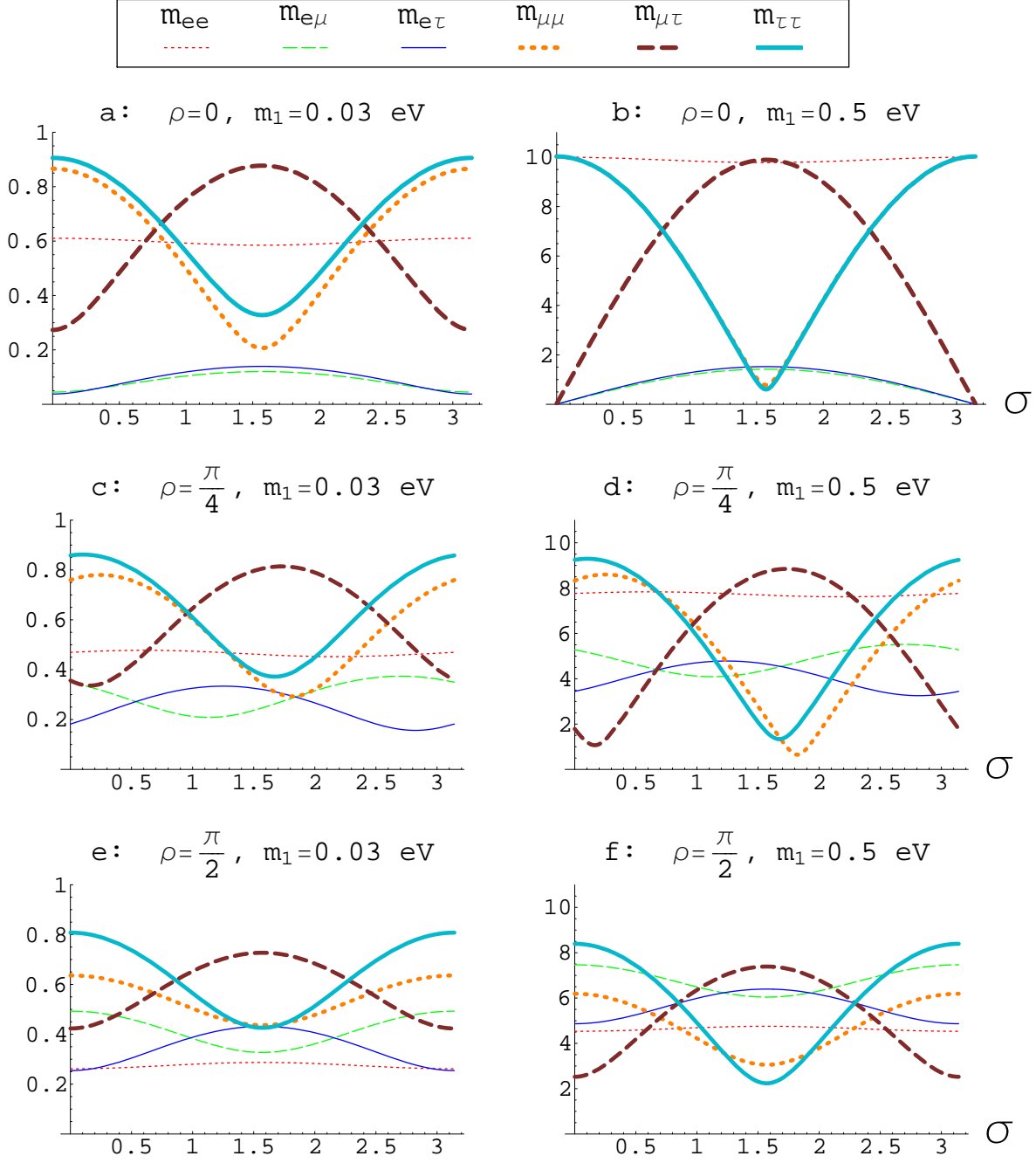


Figure 4: Dependence of the absolute value of mass matrix elements (in units  $\sqrt{\Delta m_{atm}^2}$ ) on  $\sigma$ , for partially degenerate spectrum (panels a,c,e) and completely degenerate spectrum (panels b,d,f). We show dependences for different values of the phase  $\rho$ . We take  $\Delta m_{sol}^2 = 5 \cdot 10^{-5} \text{eV}^2$ ,  $\Delta m_{atm}^2 = 2.5 \cdot 10^{-3} \text{eV}^2$  and  $\tan^2 \theta_{12} = 0.36$ ,  $\tan \theta_{23} = 0.93$ ,  $s_{13} = 0.1$ ,  $\delta = 0$ .

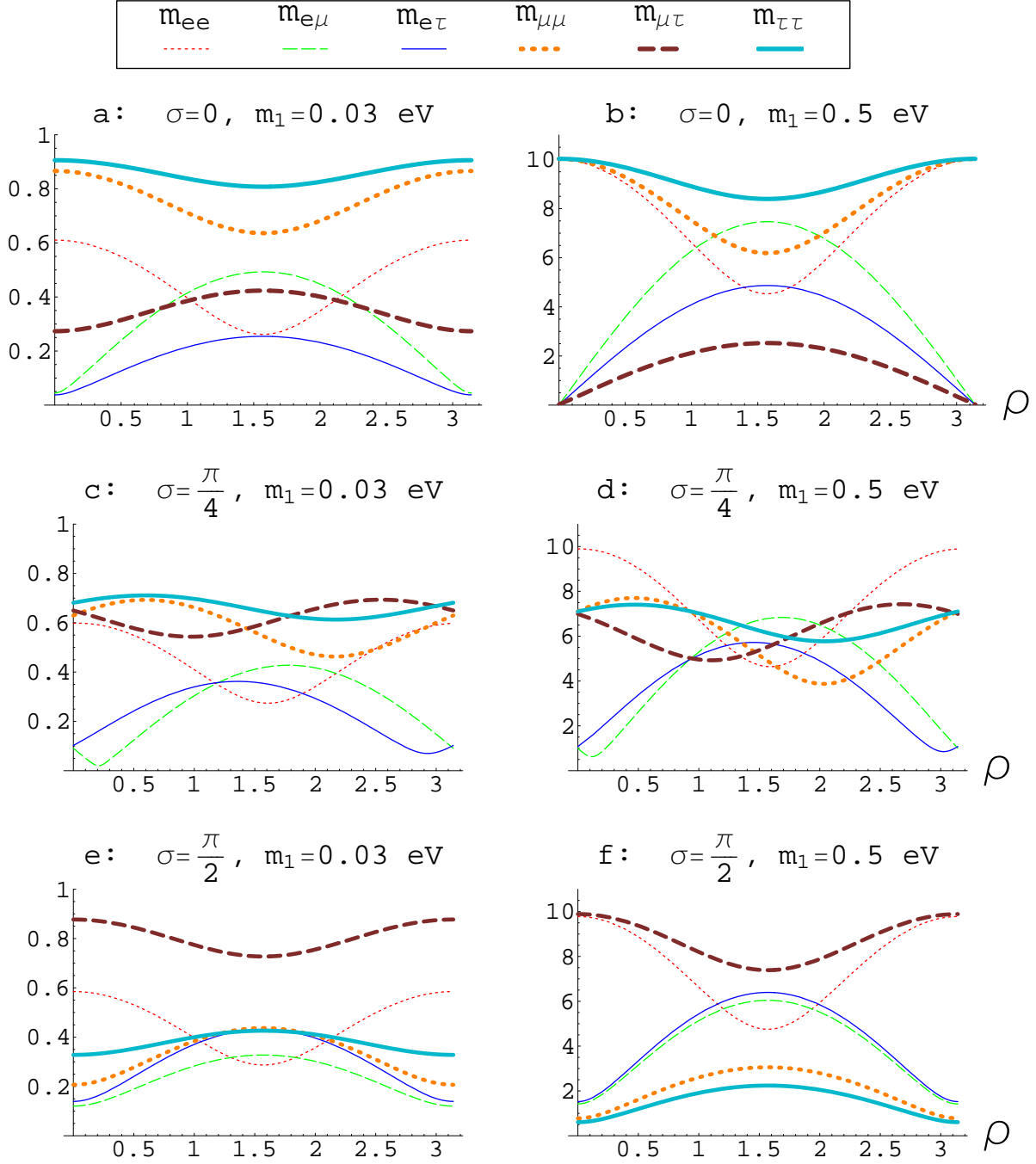


Figure 5: Dependence of the absolute value of mass matrix elements (in units  $\sqrt{\Delta m_{atm}^2}$ ) on  $\rho$ , for partially degenerate spectrum (panels a,c,e) and completely degenerate spectrum (panels b,d,f). We show dependences for different values of the phase  $\sigma$ . We take  $\Delta m_{sol}^2 = 5 \cdot 10^{-5} \text{eV}^2$ ,  $\Delta m_{atm}^2 = 2.5 \cdot 10^{-3} \text{eV}^2$  and  $\tan^2 \theta_{12} = 0.36$ ,  $\tan \theta_{23} = 0.93$ ,  $s_{13} = 0.1$ ,  $\delta = 0$ .

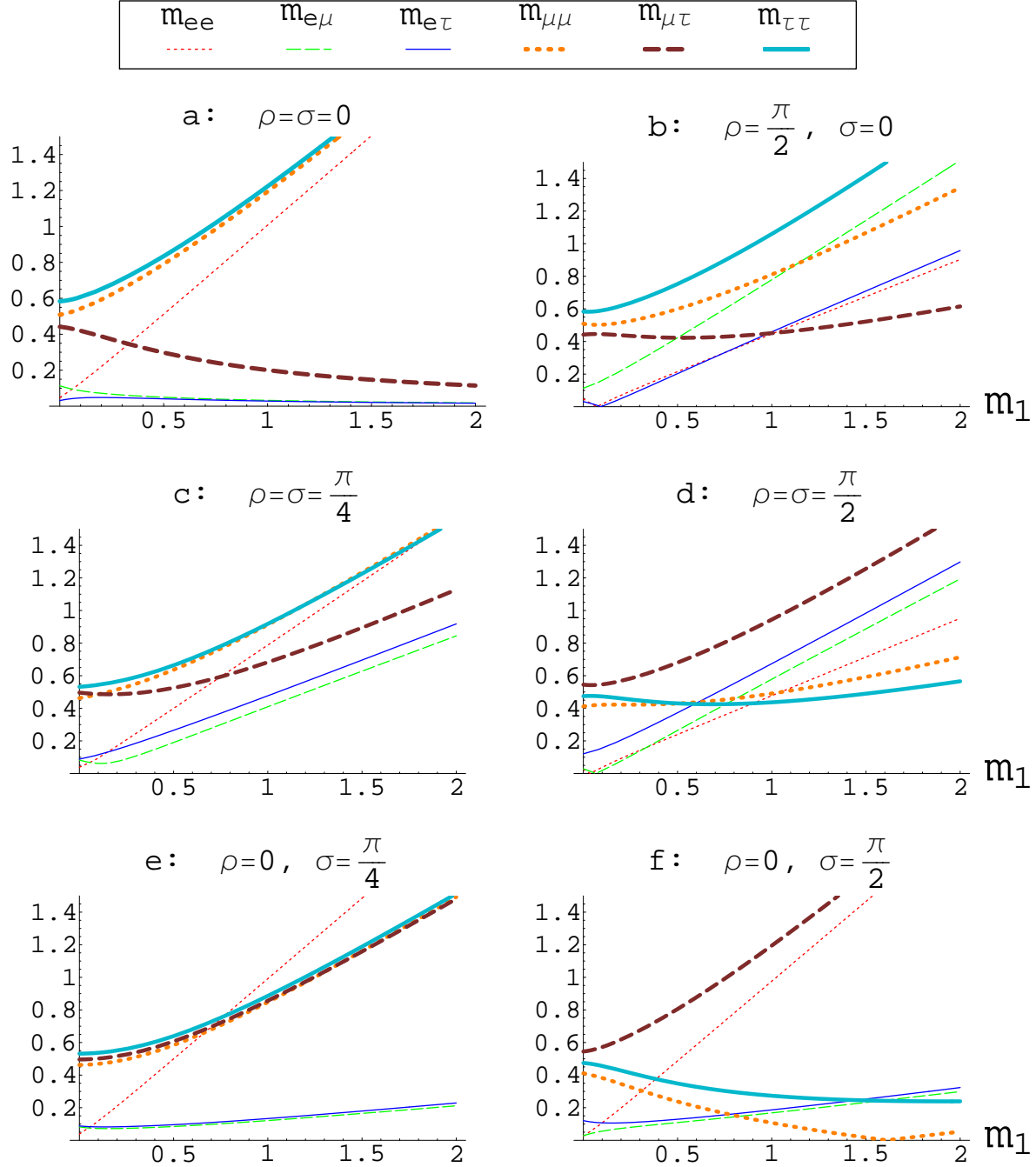


Figure 6: Dependence of the absolute value of neutrino mass matrix elements (in units  $\sqrt{\Delta m_{atm}^2}$ ) on  $m_1$ . We show dependences for different values of the phases  $\rho$  and  $\sigma$ . We take  $\Delta m_{sol}^2 = 5 \cdot 10^{-5} \text{eV}^2$ ,  $\Delta m_{atm}^2 = 2.5 \cdot 10^{-3} \text{eV}^2$  and  $\tan^2 \theta_{12} = 0.36$ ,  $\tan \theta_{23} = 0.93$ ,  $s_{13} = 0.1$ ,  $\delta = 0$ .

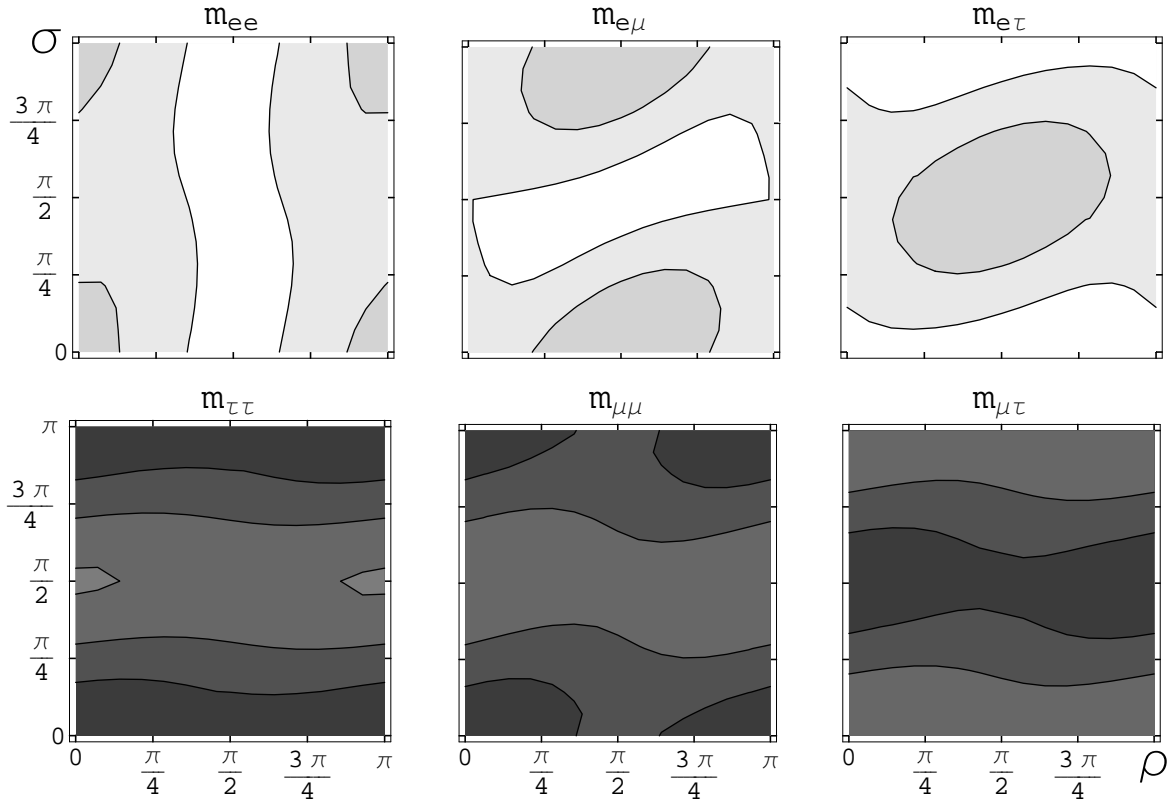


Figure 7: The  $\rho - \sigma$  plots for non-degenerate spectrum, with  $m_1 = 0.005$  eV. Shown are contours of constant mass (iso-mass)  $m = (0.1, 0.2, \dots, 0.9)m^{max}$ , where  $m^{max} = 0.03$  eV is the maximal value that the matrix elements can have, so that the white regions correspond to the mass interval  $(0 - 0.003)$  eV and the darkest ones to  $(0.027 - 0.030)$  eV. We take  $\Delta m_{sol}^2 = 5 \cdot 10^{-5} \text{eV}^2$ ,  $\Delta m_{atm}^2 = 2.5 \cdot 10^{-3} \text{eV}^2$  and  $\tan^2 \theta_{12} = 0.36$ ,  $\tan \theta_{23} = 1$ ,  $s_{13} = 0.1$ ,  $\delta = 0$ .

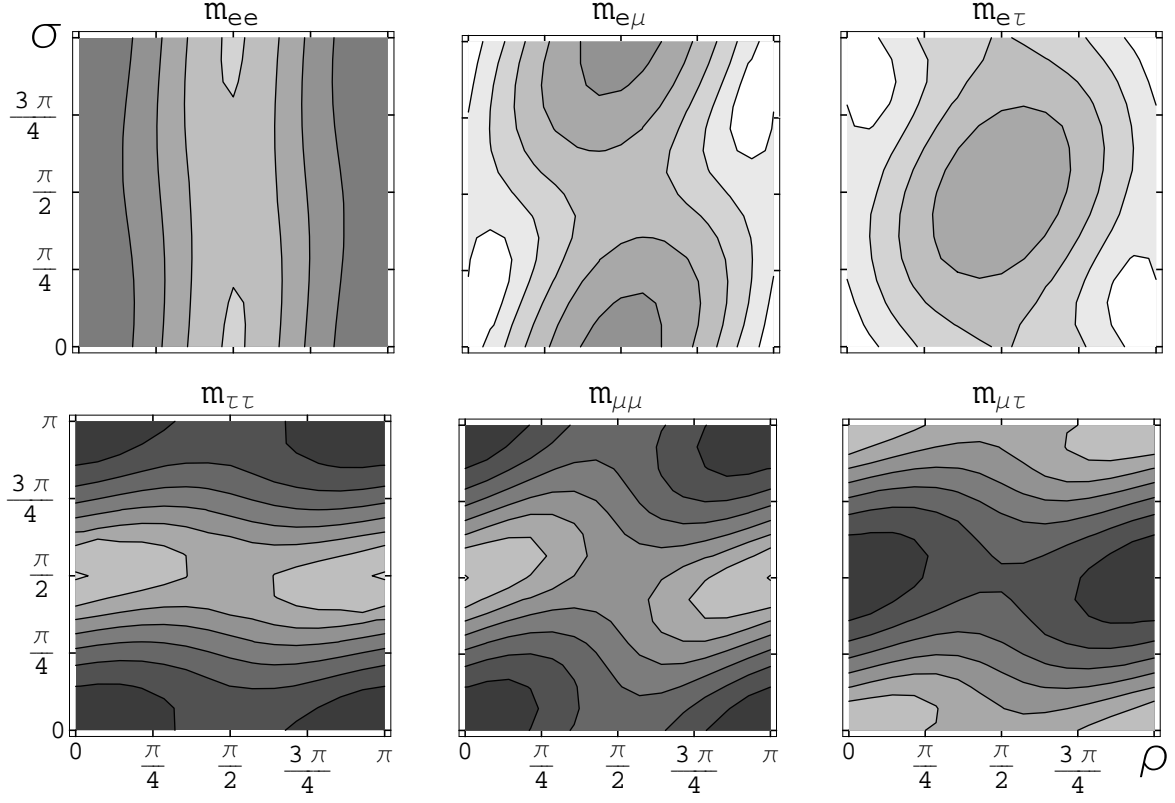


Figure 8: The  $\rho - \sigma$  plots for partially degenerate spectrum, with  $m_1 = 0.03$  eV. Shown are contours of constant mass (iso-mass)  $m = (0.1, 0.2, \dots, 0.9)m^{max}$ , where  $m^{max} = 0.045$  eV, so that the white regions correspond to the mass interval  $(0 - 0.0045)$  eV and the darkest ones to  $(0.0405 - 0.045)$  eV. We take  $\Delta m_{sol}^2 = 5 \cdot 10^{-5} \text{eV}^2$ ,  $\Delta m_{atm}^2 = 2.5 \cdot 10^{-3} \text{eV}^2$  and  $\tan^2 \theta_{12} = 0.36$ ,  $\tan \theta_{23} = 1$ ,  $s_{13} = 0.1$ ,  $\delta = 0$ .

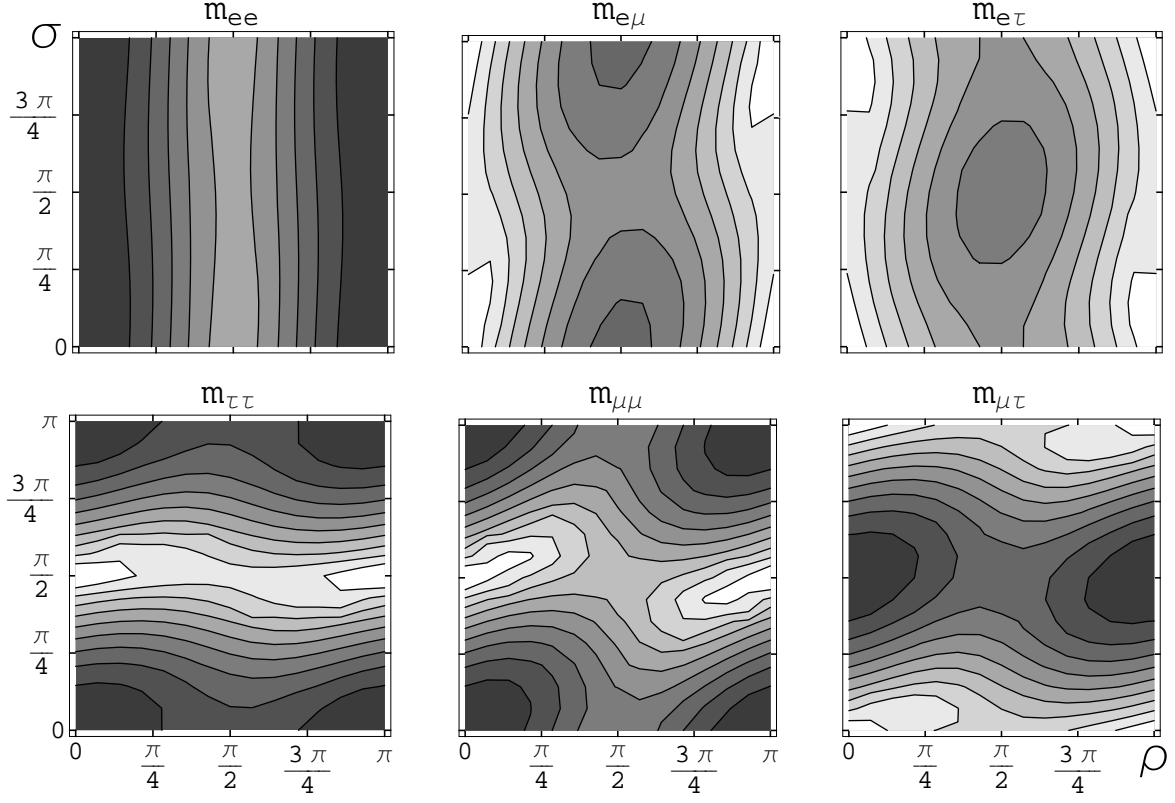


Figure 9: The  $\rho - \sigma$  plots for completely degenerate spectrum, with  $m_1 = 0.5$  eV. Shown are contours of constant mass (iso-mass)  $m = (0.1, 0.2, \dots, 0.9)m^{max}$ , where  $m^{max} = 0.5$  eV, so that the white regions correspond to the mass interval  $(0 - 0.05)$  eV and the darkest ones to  $(0.45 - 0.5)$  eV. We take  $\Delta m_{sol}^2 = 5 \cdot 10^{-5} \text{eV}^2$ ,  $\Delta m_{atm}^2 = 2.5 \cdot 10^{-3} \text{eV}^2$  and  $\tan^2 \theta_{12} = 0.36$ ,  $\tan \theta_{23} = 1$ ,  $s_{13} = 0.1$ ,  $\delta = 0$ .

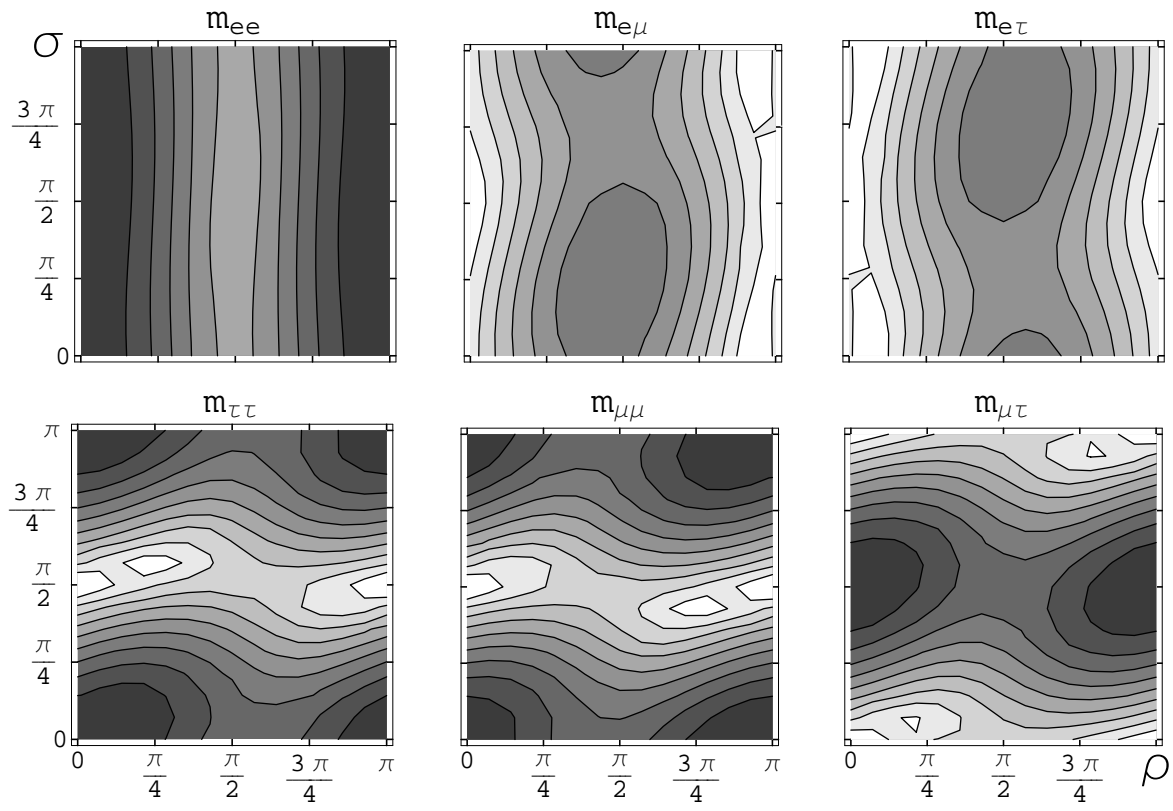


Figure 10: The same as in Fig.9, but for non-zero Dirac phase:  $\delta = \pi/2$ .



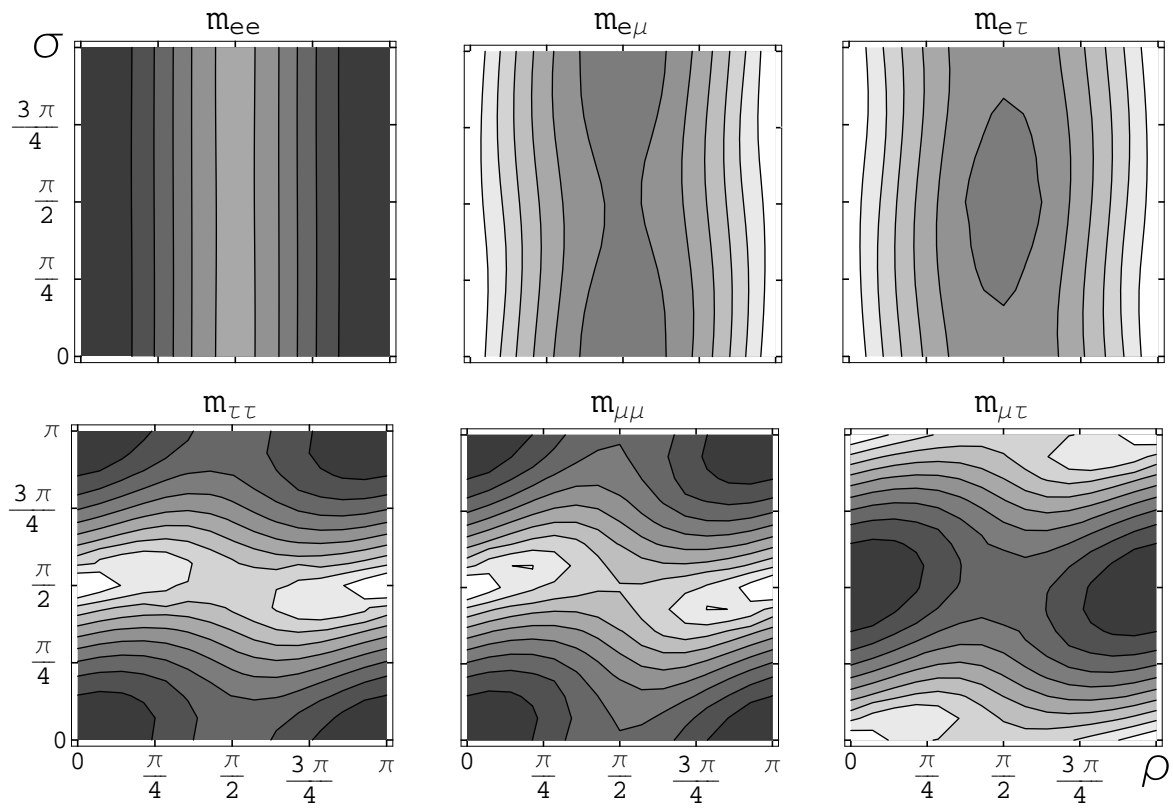


Figure 11: The same as in Fig.9, but for very small 1-3 mixing:  $\theta_{13} = 2^\circ$ .

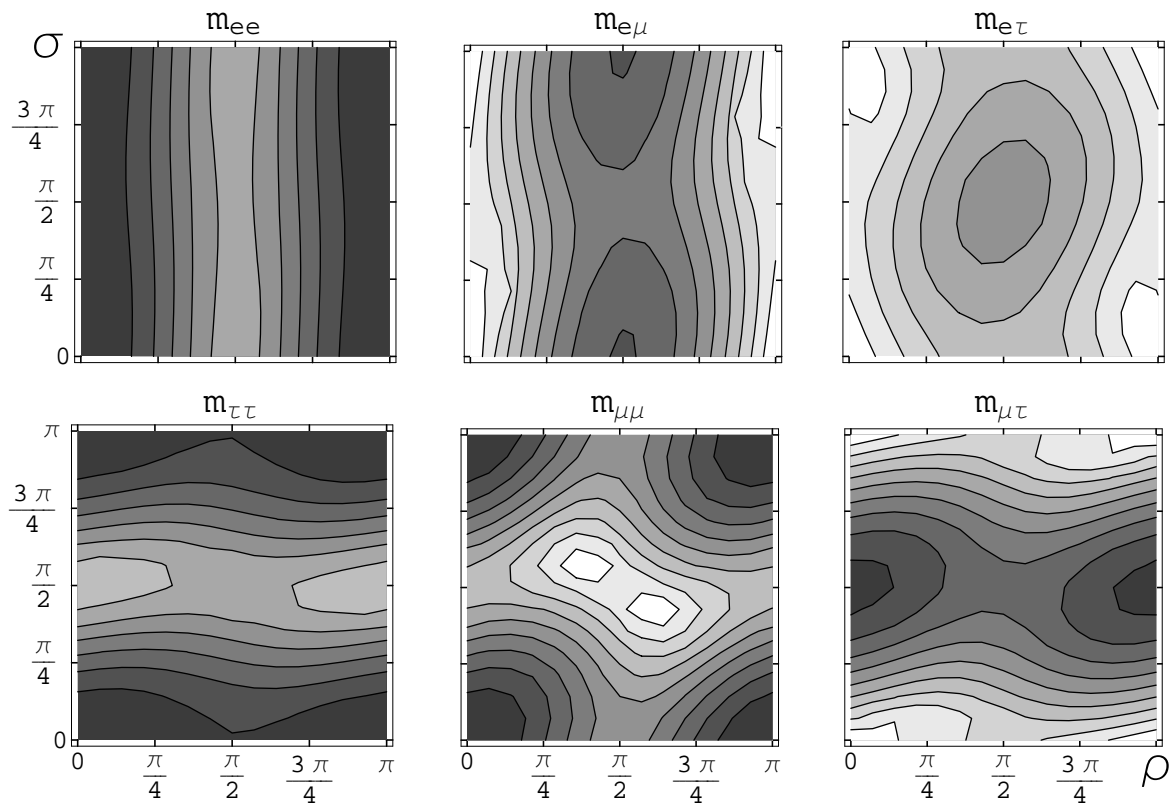


Figure 12: The same as in Fig.9, but for non-maximal 2-3 mixing:  $\theta_{23} = 35^\circ$ .

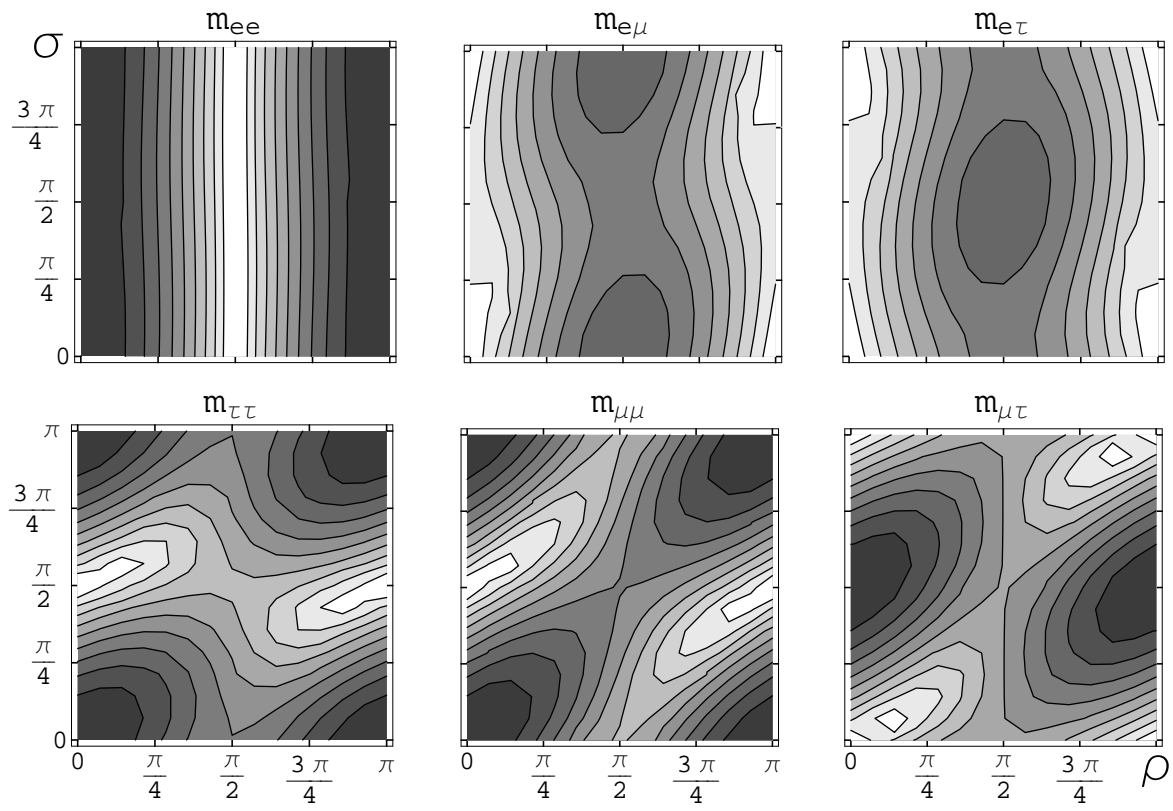


Figure 13: The same as in Fig.9, but for maximal 1-2 mixing:  $\theta_{12} = 45^\circ$ .